

Continuously varying critical exponents in long-range quantum spin ladders

Patrick Adelhardt^{1*} and Kai Phillip Schmidt^{1†}

¹ Department of Physics, Staudtstraße 7,
Friedrich-Alexander-Universität Erlangen-Nürnberg (FAU), Germany

* patrick.adelhardt@fau.de

† kai.phillip.schmidt@fau.de

January 31, 2023

1 Abstract

2 We investigate the quantum-critical behavior between the rung-singlet phase with hid-
3 den string order and the Néel phase with broken SU(2)-symmetry in quantum spin lad-
4 ders with algebraically decaying unfrustrated long-range Heisenberg interactions. To
5 this end, we determine high-order series expansions of energies and observables in the
6 thermodynamic limit about the isolated rung-dimer limit. This is achieved by extending
7 the method of perturbative continuous unitary transformations (pCUT) to long-range
8 Heisenberg interactions and to the calculation of generic observables. The quantum-
9 critical breakdown of the rung-singlet phase then allows us to determine the critical
10 phase transition line and the entire set of critical exponents as a function of the decay
11 exponent of the long-range interaction. We demonstrate long-range mean-field behavior
12 as well as a non-trivial regime of continuously varying critical exponents implying the
13 absence of deconfined criticality contrary to a recent suggestion in the literature.

14

15 Contents

16	1 Introduction	2
17	2 Model: Quantum spin ladders with long-range interactions	3
18	3 Approach: High-order series expansions with pCUT	4
19	4 Discussion of results	5
20	4.1 Quantum phase diagram	5
21	4.2 Critical exponents	6
22	5 Conclusions	9
23	A High-order series expansion	10
24	A.1 The pCUT method	10
25	A.2 Graph decomposition	11
26	A.3 Monte Carlo embedding	12
27	A.4 Derivation of physical quantities	13
28	B DlogPadé extrapolations	14
29	C Linear spin-wave calculations	15

30	D (Hyper-) scaling relations	17
31	References	18

32
33

34 1 Introduction

35 While in electromagnetism the interaction between charged particles is long-range decaying as
36 a power-law with distance, in condensed matter systems the interaction is typically screened,
37 justifying to consider short-range interactions in most microscopic investigations. There are,
38 however, notable examples where the long-range behavior persists like in conventional dipolar
39 ferromagnets [1, 2] and exotic spin-ice materials [3, 4]. In quantum optical platforms, long-
40 range interactions are commonly present and there has been tremendous experimental ad-
41 vancements over the past decades. Indeed, among others, ions in magneto-optical traps [5–16]
42 and neutral atoms in optical lattices [17–26] have gained vast attention as these platforms can
43 realize one- and two-dimensional lattices with adaptable geometries and a mesoscopic num-
44 ber of entities offering high-fidelity control and read-out. This makes them viable candidates
45 for versatile quantum simulators and scalable quantum computers [27–29]. Both platforms
46 realize effective spin interactions which decay algebraically with distance. In neutral-atom
47 platforms the decay exponent is fixed while it can be continuously tuned in trapped-ion sys-
48 tems. Recent progress ranges from the determination of molecular ground-state energies [15]
49 and the realization of equilibrium [5, 25] and dynamical quantum phase transitions [12–14]
50 to the direct observation of a symmetry-protected topological phase [22] or a topologically-
51 ordered quantum spin liquid [26].

52 The majority of numerical studies has focused on one-dimensional spin chains [30–40,
53 40–46, 46–52] as well as two-dimensional systems directly related to Rydberg atom platforms
54 with quickly decaying ($\sim r^{-6}$) long-range interactions [53–55]. One prominent exception is
55 the long-range transverse-field Ising model (LRTFIM), which was recently analyzed on the two-
56 dimensional square and triangular lattice with tunable long-range interactions [56–58]. Geo-
57 metrically unfrustrated LRTFIMs in one and two dimensions are known from field-theoretical
58 considerations to display three distinct regimes of quantum criticality between the high-field
59 polarized phase and the low-field \mathbb{Z}_2 -symmetry broken ground state: For short-range interac-
60 tions the system exhibits nearest-neighbor criticality, for strong long-range interactions long-
61 range mean-field behavior, and in-between continuously varying critical exponents [59–64].

62 Less is known about the quantum-critical behavior of systems with long-range interactions
63 possessing a continuous symmetry. Here, the antiferromagnetic spin-1/2 Heisenberg model
64 is the most prominent example where, however, only the one-dimensional chain has been
65 investigated microscopically [35, 41, 42, 45, 47, 65]. For the short-range Heisenberg chain,
66 the spontaneous breaking of its continuous $SU(2)$ -symmetry is forbidden by the Hohenberg-
67 Mermin-Wagner (HMW) theorem [66–70] and the system displays quasi long-range order with
68 gapless fractional spinon excitations. The HMW theorem can be circumvented when unfrus-
69 trated long-range interactions are sufficiently strong, giving rise to a quantum phase transition
70 to a Néel state with broken $SU(2)$ -symmetry [35, 40–42, 45, 47, 65]. Interestingly, beyond the
71 chain geometry, a recent work [71] has studied an antiferromagnetic quasi one-dimensional
72 two-leg quantum spin ladder with unfrustrated long-range Heisenberg interactions. Here,
73 an exotic deconfined quantum critical point between the gapped short-range isotropic ladder
74 with a non-local string order parameter and the Néel state with broken $SU(2)$ -symmetry has
75 been suggested [71]. The proposed transition goes therefore even beyond the established

76 scenario of deconfined quantum criticality between two ordered phases with local order pa-
77 rameters [72–76].

78 In this paper, we investigate two types of long-range quantum spin ladders with arbitrary
79 ratios λ of nearest-neighbor leg and rung exchange coupling and for arbitrary decay exponent
80 $1 + \sigma$ of the long-range Heisenberg interaction. To this end, we extend the pCUT approach
81 developed in Ref. [57] to generic observables and locate the critical breakdown of the rung-
82 singlet phase in the $\sigma - \lambda$ parameter plane. This allows us to observe long-range mean-field
83 behavior as well as a non-trivial regime of continuously varying critical exponents. We stress
84 that the model studied in Ref. [71] is contained as one specific parameter line $\lambda = 1$ in our two-
85 dimensional quantum phase diagram. From our findings and physical arguments we conclude
86 that the investigated long-range Heisenberg quantum spin ladders do not show deconfined
87 criticality.

88 2 Model: Quantum spin ladders with long-range interactions

89 We consider the spin-1/2 Hamiltonian

$$\mathcal{H} = J_{\perp} \sum_i \vec{S}_{i,1} \vec{S}_{i,2} - \sum_{i,\delta>0} \sum_{n=1}^2 J_{\parallel}(\delta) \vec{S}_{i,n} \vec{S}_{i+\delta,n} - \sum_{i,\delta>0} J_{\times}(\delta) (\vec{S}_{i,1} \vec{S}_{i+\delta,2} + \vec{S}_{i,2} \vec{S}_{i+\delta,1}), \quad (1)$$

90 where the indices i and $i + \delta$ denote the rung and the second index $n \in \{1, 2\}$ the leg of the
91 ladder. The exchange parameters $J_{\perp} > 0$,

$$J_{\parallel}(\delta) = J_{\parallel} \frac{(-1)^{\delta}}{|\delta|^{1+\sigma}}, \quad J_{\times}(\delta) = J_{\times} \frac{(-1)^{1+\delta}}{|1 + \delta|^{1+\sigma}}, \quad (2)$$

92 couple spin operators on the rungs, legs, and diagonals, respectively. The distant-dependent
93 coupling parameters $J_{\parallel}(\delta)$ and $J_{\times}(\delta)$ realize unfrustrated algebraically decaying long-range
94 interactions which induce antiferromagnetic Néel order for sufficiently small σ . This decay
95 exponent σ can be tuned between the limiting cases of all-to-all interactions at $\sigma = -1$ and
96 nearest-rung couplings at $\sigma = \infty$. Here, we focus on $\sigma \geq 0$ so that the energy of the system
97 is extensive in the thermodynamic limit. We restrict to the limiting cases $\mathcal{H}_{\parallel} \equiv \mathcal{H}|_{J_{\times}=0}$ and
98 $\mathcal{H}_{\times} \equiv \mathcal{H}|_{J_{\parallel}=J_{\parallel}}$ illustrated in Fig. 1. In the following, we set $J_{\perp} = 1$ and introduce the pertur-
99 bation parameter $\lambda \equiv J_{\parallel}$. Note, the Hamiltonian in Ref. [71] corresponds to \mathcal{H}_{\times} at $\lambda = 1$. In
100 the limit of isolated rung dimers $\lambda = 0$, the ground state is given exactly by the product state
101 of rung singlets

$$|s\rangle = \frac{1}{\sqrt{2}} (|\uparrow\downarrow\rangle - |\downarrow\uparrow\rangle) \quad (3)$$

102 and with localized rung triplets

$$|t_x\rangle = -\frac{1}{\sqrt{2}} (|\uparrow\uparrow\rangle - |\downarrow\downarrow\rangle), \quad |t_y\rangle = \frac{i}{\sqrt{2}} (|\uparrow\uparrow\rangle + |\downarrow\downarrow\rangle), \quad |t_z\rangle = \frac{1}{\sqrt{2}} (|\uparrow\downarrow\rangle + |\downarrow\uparrow\rangle) \quad (4)$$

103 as elementary excitations. For small λ the ground state is adiabatically connected to this prod-
104 uct state and the system is in the rung-singlet phase. The associated elementary excitations
105 of the rung-singlet phase are gapped triplons [77] corresponding to dressed rung-triplet ex-
106 citations. For $\sigma = \infty$ this holds for both spin ladders for any finite λ and only at $\lambda = \infty$
107 the system decouples into two spin-1/2 Heisenberg chains with gapless spinon excitations and
108 a quasi long-range ordered ground state. The ground states at any finite λ break a hidden
109 $\mathbb{Z}_2 \times \mathbb{Z}_2$ symmetry and can be characterized by a non-local string order parameter [78–82].

110 Previous studies of the spin-1/2 Heisenberg chain [40–42, 45] and the two-leg ladder \mathcal{H}_{\times}

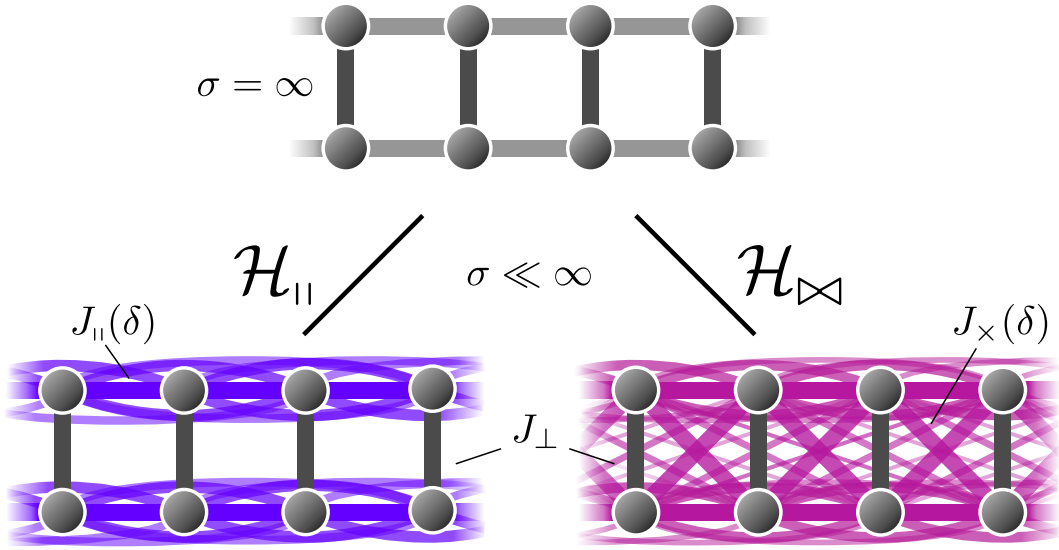


Figure 1: Illustration of the two quantum spin ladders with Heisenberg interaction on rung dimers ($\sim J_{\perp}$), between rung dimers along the legs ($\sim J_{\parallel}$) and along the diagonals ($\sim J_{\times}$). In the first row the common nearest-neighbor limit ($\sigma = \infty$) of both ladder models is shown while in the second row the two distinct spin ladders \mathcal{H}_{\parallel} (left) and \mathcal{H}_{\times} (right) with long-range interactions $\sigma \ll \infty$ are sketched.

111 for $\lambda = 1$ [71] with unfrustrated long-range interactions deduced a quantum phase tran-
 112 sition towards Néel order with broken $SU(2)$ -symmetry and thus circumventing the HMW
 113 theorem [66–70]. Further, Goldstone’s theorem states that the spontaneous breaking of a
 114 continuous symmetry gives rise to massless Nambu-Goldstone modes [83–85], however, the
 115 same restriction applies and the theorem loses its validity in the presence of long-range inter-
 116 actions. Indeed, in the extreme case of an all-to-all coupling the ground-state energy becomes
 117 superextensive and the elementary excitations are gapped via a generalization of the Higgs
 118 mechanism [86].

119

120 3 Approach: High-order series expansions with pCUT

121 Our aim is to investigate the quantum critical breakdown of the rung-singlet phase. To this
 122 end, we extend the pCUT method [87, 88] to long-range Heisenberg interactions and deter-
 123 mine high-order series expansions of relevant energies and observables in the thermodynamic
 124 limit about the limit of isolated rungs. It is then convenient to consider rung dimers as super-
 125 sites and to reformulate the Hamiltonian (1) in terms of hard-core bosonic triplet creation and
 126 annihilation operators on rung dimers.

127 The pCUT method transforms the original Hamiltonian \mathcal{H} , perturbatively order by order
 128 in λ , into an effective Hamiltonian \mathcal{H}_{eff} conserving the number of quasiparticles (QPs) which
 129 correspond to spin-one triplon excitations [77] - dressed rung triplets - in the rung-singlet
 130 phase. The same transformation has to be applied for observables, however, the quasiparticle-
 131 conserving property is lost. We can exploit the linked-cluster property [89] and perform the
 132 numerical calculations on finite topologically distinct graphs. In the end, the contributions on
 133 the finite graphs must be embedded on an infinite system to obtain the bulk properties which is
 134 equivalent to evaluating high-dimensional infinite sums that can be efficiently done by Monte

135 Carlo integration [57].

136 Here, we investigate the zero- and one-triplon properties. The 0QP block of the effective
137 Hamiltonian corresponds to the ground-state energy \bar{E}_0 while the 1QP block allows the calcula-
138 tion of the one-triplon gap Δ located at the critical momentum $k_c = \pi$. Further, we extended
139 the pCUT approach for long-range interactions [57] to generic observables and determined
140 the one-triplon spectral weight $S^{1\text{QP}}(k_c)$. The latter corresponds to the one-triplon part of the
141 Fourier transformed effective observable after the unitary transformation of the antisymmetric
142 observable

$$O_{i,z} = \frac{1}{2}(S_{i,1}^z - S_{i,2}^z) \quad (5)$$

143 on a rung dimer. We calculated high-order series of the control-parameter susceptibility $\chi \equiv \frac{d^2 \bar{E}_0}{d\lambda^2}$
144 up to order 10 (6), the one-triplon gap Δ up to order 10 (7), and the one-triplon spectral
145 weight $S^{1\text{QP}}(k_c)$ up to order 9 (7) in λ for \mathcal{H}_{\parallel} (\mathcal{H}_{\bowtie}). See Appendix A for details on the pCUT
146 approach.

147 The introduced quantities allow the extraction of critical exponents via the dominant
148 power-law behavior

$$\chi \sim |\lambda - \lambda_c|^{-\alpha}, \quad (6)$$

$$\Delta \sim |\lambda - \lambda_c|^{z\nu}, \quad (7)$$

$$S^{1\text{QP}}(k_c) \sim |\lambda - \lambda_c|^{-(2-z-\eta)\nu} \quad (8)$$

149 close to the critical point λ_c when the rung-singlet phase breaks down. The critical point and
150 associated critical exponents can be directly determined from physical poles and associated
151 residuals using (biased) DlogPadé extrapolants. The associated error bars should strictly be
152 understood as the standard deviation from several extrapolants rather than rigorous errors.
153 More detailed information on extrapolations can be found in Appendix B.

154 4 Discussion of results

155 4.1 Quantum phase diagram

156 We determine the phase transition point λ_c as a function of the decay exponent σ by the
157 quantum-critical breakdown of the rung-singlet phase and the accompanied closing of the one-
158 triplon gap. The corresponding quantum phase diagram is shown in Fig. 2 for \mathcal{H}_{\parallel} and \mathcal{H}_{\bowtie} . In
159 accordance with the HMW theorem, a quantum phase transition can be ruled out from one-
160 loop renormalization group (RG) for $\sigma > 2$ [59], since the one-dimensional $O(3)$ quantum
161 rotor model can be mapped to the low-energy physics of the dimerized antiferromagnetic
162 Heisenberg ladder [90]. At small $\sigma \lesssim 0.7$ ($\sigma \lesssim 1.0$) for \mathcal{H}_{\parallel} (\mathcal{H}_{\bowtie}) the critical point λ_c shifts
163 linearly towards larger λ with increasing σ . The gap closes earlier for \mathcal{H}_{\bowtie} in agreement with
164 expectations since the additional diagonal interactions further stabilize the antiferromagnetic
165 Néel order. For larger σ the critical points start to deviate from the linear behavior and bend
166 upwards towards larger critical points until eventually DlogPadé extrapolations break down
167 when the critical point shifts away significantly from the radius of convergence of the series.

168 We complement the pCUT approach with linear spin-wave calculations similar the ones
169 in Refs. [41, 42]. Exploiting the fact that spin-wave theory is expected to work only in the
170 Néel ordered phase, we can determine the quantum-critical line from a consistency condition
171 for the staggered magnetization (see also Appendix C). Linear spin-wave theory allows us to
172 qualitatively determine the extent of the Néel ordered phase in the whole parameter regime.
173 Indeed, we find for small λ that linear spin-wave theory agrees well with the pCUT findings

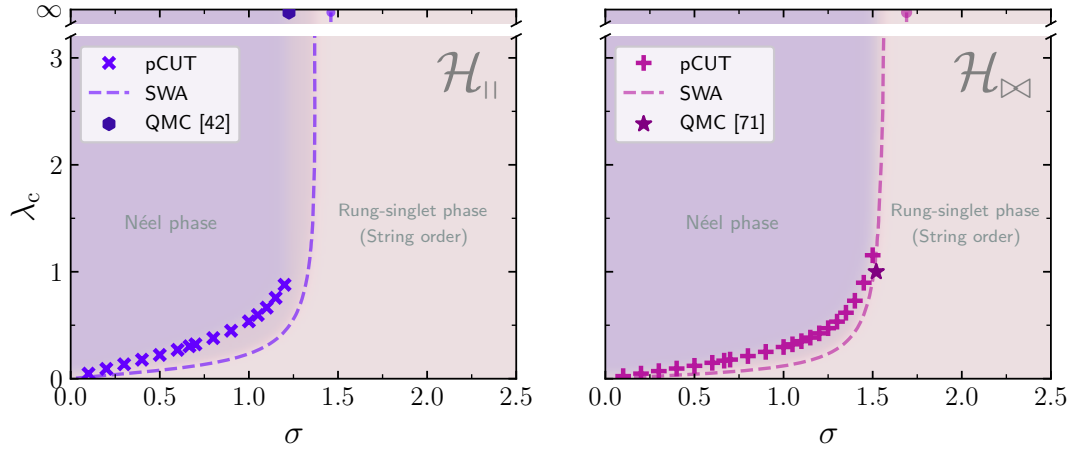


Figure 2: Quantum phase diagrams depicting the critical point λ_c as a function of the decay exponent σ for $\mathcal{H}_{||}$ (left) and \mathcal{H}_{\perp} (right). Crosses are determined by DlogPadé extrapolations of the one-triplon gap series from the pCUT method while dashed lines are extracted from the self-consistency condition for the staggered magnetization within linear spin-wave approximation (SWA). Comparing the left with the right plot, we observe that the Néel ordered phase sets in at smaller λ or larger σ exponents extending the Néel regime. The hexagon point at $\lambda = \infty$ for $\mathcal{H}_{||}$ corresponding to decoupled Heisenberg chains from Ref. [42] as well the star-shaped point along the $\lambda = 1$ line for \mathcal{H}_{\perp} from Ref. [71] are consistent with our results.

174 and we also observe that the Néel regime extends to smaller λ and larger σ for \mathcal{H}_{\perp} due to
 175 the additional diagonal interactions. In the limit $\lambda = \infty$ of decoupled Heisenberg chains
 176 where the pCUT series expansion does not provide any meaningful results we locate an upper
 177 critical bound σ_* inline with the absence of criticality at large enough σ . This upper bound
 178 corresponds therefore to the lower critical dimension. In fact, for $\mathcal{H}_{||}$ at $\lambda = \infty$ we recover
 179 the spin-wave dispersion in Ref. [42] yielding $\sigma_*^{SW} \approx 1.46$ and for \mathcal{H}_{\perp} we find $\sigma_*^{SW} \approx 1.69$.

180 Moreover, all our data is consistent with $\sigma_* = 1.225(25)$ at $\lambda = \infty$ from Ref. [42] for $\mathcal{H}_{||}$
 181 and with $\sigma_c \approx 1.52$ at $\lambda_c = 1$ for \mathcal{H}_{\perp} in Ref. [71] as depicted in Fig. 2. Besides this, the critical
 182 exponents in the long-range mean-field realm discussed below are in very good agreement with
 183 field-theoretical expectations. However, the distinct values for σ_* from spin-wave calculations
 184 and QMC [42] consistent with the pCUT results for both ladder models are unexpectedly at
 185 significant smaller values than predicted from the one-dimensional long-range $O(3)$ quantum
 186 rotor model with $\sigma_* = 2$ [60, 61, 91, 92].

187 4.2 Critical exponents

188 We extract the critical exponents according to Eqs. (6)-(8) from DlogPadé extrapolants of the
 189 perturbative series. The exponents are depicted in Fig. 3 as a function of the decay exponent
 190 σ . The long-range mean-field regime (LRMF) is expected to extend to $\sigma_{uc} = 2/3$ [59]. The
 191 extracted exponents agree well with expected long-range mean-field exponents, although the
 192 presence of multiplicative logarithmic corrections to the dominant power-law behavior at the
 193 upper critical dimension $d_{uc} = 3\sigma/2$ negatively affects the accuracy of the deduced critical
 194 exponents around $\sigma = 2/3$ as known from the LRFTIM [37, 57]. Estimates for multiplicative
 195 logarithmic critical exponents can be found in Appendix B. Excluding the α -exponent the crit-
 196 ical exponents deviate less than 1.1% (1.3%) deep in the long-range regime $\sigma \leq 0.3$ for $\mathcal{H}_{||}$
 197 (\mathcal{H}_{\perp}). For $\sigma > 2/3$ we observe continuously varying exponents which seem to diverge for

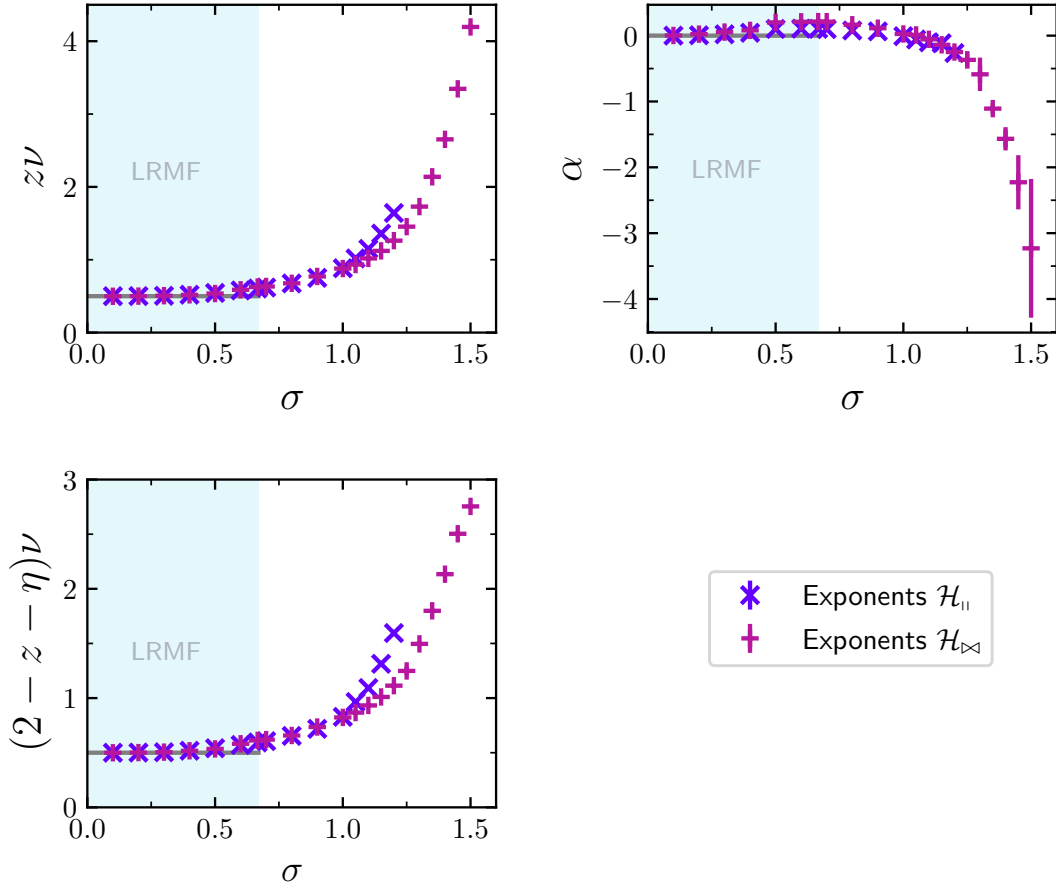


Figure 3: Critical exponents from Eqs. (6)-(8) determined by the pCUT approach as a function of the decay exponent σ for both ladder models $\mathcal{H}_{||}$ and \mathcal{H}_{∞} . For $\sigma \leq 2/3$ the exponents coincide with the expected long-range mean-field values (shaded region). For $\sigma > 2/3$ they become continuously larger and start to diverge. While the critical exponent for both models match well for $\sigma \lesssim 2.1$, they start to deviate from each other for larger values of σ but this can probably be attributed to the difference in σ_* .

198 $\sigma \rightarrow \sigma_*$. In terms of the gap closing this can be understood from the nearest-neighbor limit
 199 where the gap does not close but with the increasingly stronger long-range interactions the
 200 finite gap is lowered until eventually the gap closes. Further strengthening the long-range in-
 201 teractions shifts the critical point from infinity to smaller values and thus continuously tuning
 202 the exponent $z\nu$ from infinity to smaller values as the gap closes increasingly steep. In the
 203 region $\sigma \gtrsim 1.1$ for $\mathcal{H}_{||}$ ($\sigma \gtrsim 1.2$ for \mathcal{H}_{∞}) close to σ_* it becomes difficult to extrapolate the gap
 204 series as the critical point starts to shift quickly towards $\lambda = \infty$. This negatively affects the
 205 accuracy of the exponent estimates.

206 Using the three critical exponents shown Fig. 3, one can apply the scaling relations

$$\begin{aligned}
 \gamma &= (2 - \eta)\nu \\
 \gamma &= \beta(\delta - 1), \\
 2 &= \alpha + 2\beta + \gamma
 \end{aligned} \tag{9}$$

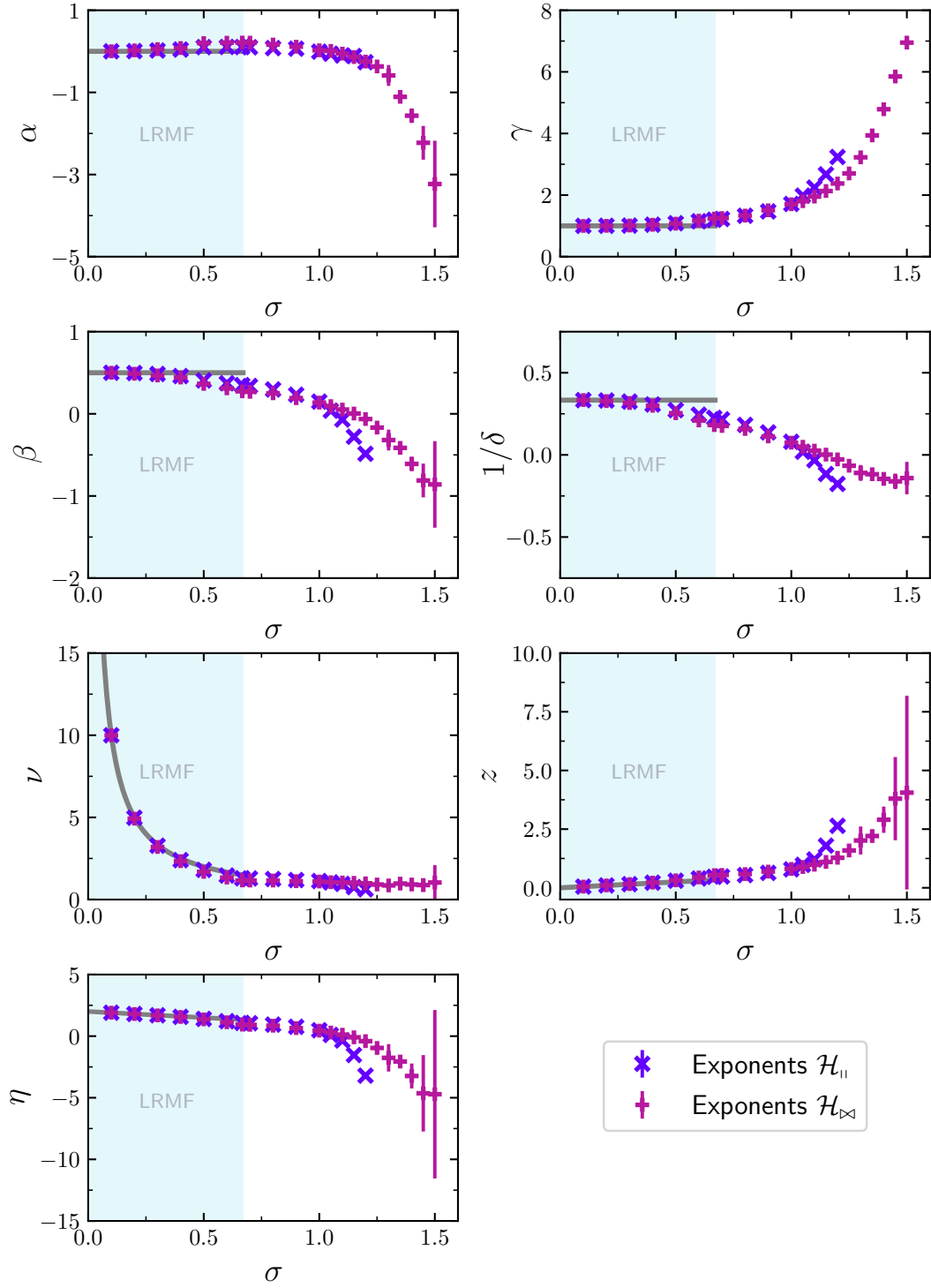


Figure 4: Canonical critical exponents obtained from (hyper-) scaling relations as a function of the decay exponent σ . The critical exponents are in good agreement with expectations in the long-range mean-field regime (shaded region) and show continuously varying exponents for $\sigma > 2/3$. While some critical exponents appear to diverge others seem to go to a constant value for increasing σ . For some exponents the error bars become larger for $\sigma \approx \sigma_*$.

207 as well as the hyperscaling relation

$$2 - \alpha = \left(\frac{d}{\varrho} + z \right) \nu \quad (10)$$

208 with the pseudocritical exponent ϱ . The hyperscaling relation was only recently generalized to
 209 be valid above the upper critical dimension [39]. This allows us to directly derive all canonical
 210 critical exponents for any σ (see Appendix D). The canonical critical exponents are depicted
 211 in Fig. 4 for \mathcal{H}_{\parallel} and \mathcal{H}_{\bowtie} . In the long-range mean-field regime the exponents agree well with
 212 the expectations. The exponents β and $1/\delta$ around the upper critical dimension show larger
 213 deviations which we attribute to error propagation due to the presence of multiplicative loga-
 214 rithmic corrections. While the critical exponent γ diverges for larger values of σ , the critical
 215 exponent ν approaches a constant value $\nu \approx 1$. The exponent $1/\delta$ goes to -0.125 in this limit
 216 and we attribute this to a systematic error arising from the diverging critical exponents close
 217 to σ_* . Instead, the correct physical limit might be 0 since a sign change of $1/\delta$ is unphysical.
 218 For the exponents β , z and η the uncertainty in the regime $\sigma \gtrsim 1.2$ becomes large due to
 219 error propagation and it is hard to make precise statements in the vicinity of σ_* . Nonethe-
 220 less, we find that η differs from the linear behavior $\eta = 2 - \sigma$ expected by field theory for
 221 $\sigma < \sigma_*$ [60, 91, 92] going faster to zero (until unphysically negative values are obtained) but
 222 in agreement with our previous finding that σ_* is smaller than expected by the long-range
 223 $O(3)$ quantum rotor model.

224 Comparing the above results with Ref. [71] for \mathcal{H}_{\bowtie} at $\lambda = 1$ we find that the exponent
 225 $\nu = 1.8$ at about $\sigma_c \approx 1.5$ is inconsistent with our result $\nu = 0.97(7)$ for all $\sigma > 1.0$ which ap-
 226 pears to be particularly well converged compared to other critical exponents. Furthermore, the
 227 monotonously increasing exponent $z > 1$ for $\sigma > 1.1$ is not in line with a proposed deconfined
 228 critical point with $z = 1$ at $\sigma \approx 1.5$. Our finding of continuously varying exponents reminis-
 229 cent of the criticality of the unfrustrated LRTFIM [37, 57, 59–64] raises the question why this
 230 specific point should display deconfined criticality, particularly considering that despite the
 231 presence of a non-local string order parameter the rung singlet-phase of both models \mathcal{H}_{\parallel} and
 232 \mathcal{H}_{\bowtie} for all relevant λ is not topologically protected but trivially connected to the product state
 233 of rung singlets [93].

234 5 Conclusions

235 We investigated the quantum-critical behavior of two unfrustrated two-leg quantum spin lad-
 236 ders with long-range Heisenberg interactions by applying and extending the pCUT method in
 237 combination with classical Monte Carlo integration that allows us to determine relevant ener-
 238 gies and observables in the thermodynamic limit. From the closing of the one-triplon gap we
 239 determined the phase diagram in the $\sigma - \lambda$ plane for both spin ladders. Interestingly, we find
 240 lower critical dimensions $\sigma_* < 2$ unlike $\sigma_* = 2$ from field-theoretical predictions for the one-
 241 dimensional long-range $O(3)$ quantum rotor model, but in agreement with known results [42]
 242 from the isolated chain limit. By generalizing the pCUT approach for long-range systems to
 243 generic observables, we calculated the ground-state energy and the one-triplon spectral weight
 244 so that we were able to extract the full set of critical exponents as a function of the decay expo-
 245 nent using appropriate extrapolation techniques. A non-trivial regime of continuously varying
 246 critical exponents as well as long-range mean-field behavior was observed. From these find-
 247 ings and the fact that the rung-singlet phase is not topologically protected we conclude the
 248 absence of deconfined criticality in the investigated models. However, quantum phase transi-
 249 tions between phases with local order and non-local string order parameters, where the latter
 250 phase is indeed topologically protected, should be investigated in the future as such systems

251 might realize exotic properties like deconfined criticality. The spin-one Heisenberg chain with
 252 unfrustrated long-range interactions should therefore be very interesting to look at. Our ap-
 253 proach can further be naturally extended to gapped phases of higher-dimensional Heisenberg
 254 systems with long-range interactions, e.g., bilayer geometries. This opens a completely unex-
 255 plored playground for future research.

256

257 Acknowledgements

258 P.A. and K.P.S. thank M. Mühlhauser for providing the graph files, J. A. Koziol for fruitful dis-
 259 cussions and thankfully acknowledge the scientific support and HPC resources provided by
 260 the Erlangen National High Performance Computing Center (NHR@FAU) of the Friedrich-
 261 Alexander-Universität Erlangen-Nürnberg (FAU).

262 **Funding information** We gratefully acknowledge the support by the Deutsche Forschungsge-
 263 meinschaft (DFG, German Research Foundation) – Project-ID 429529648—TRR 306 QuCoLiMa
 264 (“Quantum Cooperativity of Light and Matter”) as well as the Munich Quantum Valley, which
 265 is supported by the Bavarian state government with funds from the Hightech Agenda Bayern
 266 Plus. The hardware of NHR@FAU is funded by the German Research Foundation DFG.

267 **Author contributions** P.A. performed the spin-wave calculations and the numerical simula-
 268 tions. P.A. analyzed the results with assistance from K.P.S. who supervised the project. Both
 269 authors contributed equally to the writing of the manuscript.

270 **Data availability** The raw data is available on Zenodo at: <http://url>. The code used to gen-
 271 erate the numerical results presented in this paper can be made available by Patrick Adelhardt
 272 (patrick.adelhardt@fau.de) upon reasonable request.

273 **Competing interests** The authors declare no competing interests.

274 A High-order series expansion

275 In the following, we provide a description of the high-order series expansions approach using
 276 the pCUT method along the same lines as in previous studies on the LRTFIM [38, 39, 57, 94].
 277 The approach can be generalized to observables which allows us to determine the entire set
 278 of critical exponents.

279 A.1 The pCUT method

280 To apply the pCUT method [87, 88] it must be possible to describe the problem under consid-
 281 eration with a Hamiltonian of the form

$$\mathcal{H} = \mathcal{H}_0 + \mathcal{V} = E_0 + \mathcal{Q} + \sum_{\delta > 0}^{\infty} \lambda(\delta) \mathcal{V}(\delta) \quad (11)$$

282 with an unperturbed Hamiltonian \mathcal{H}_0 with equidistant spectrum that is bounded from be-
 283 low and a perturbation \mathcal{V} . We bring the spin-ladder Hamiltonian into this form by inter-
 284 preting the Hamiltonian as a system of coupled supersites (dimers) and introducing hard-
 285 core bosonic triplet (creation) annihilation operators $t_{i,\rho}^{(\dagger)}$ (creating) annihilating local triplets

286 with flavor $\rho \in \{x, y, z\}$ on rung i [95, 96]. The unperturbed part becomes $\mathcal{H}_0 = E_0 + \mathcal{Q}$
 287 with $E_0 = -3/4N_{\text{rung}}$ the unperturbed ground-state energy, N_{rung} the number of rungs, and
 288 $\mathcal{Q} = \sum_{i,\rho} t_{i,\rho}^\dagger t_{i,\rho}$ counting the number of triplet quasiparticles (QPs). For long-range systems
 289 the perturbation \mathcal{V} can be written as a sum between interacting processes of distance δ with a
 290 distance-dependent expansion parameter $\lambda(\delta)$. Also, the perturbation must decompose into

$$\mathcal{V} = \sum_{m=-N}^N T_m = \sum_{m=-N}^N \sum_l \tau_{m,l}, \quad (12)$$

291 where the operators T_m change the system's energy by m energy quanta such that $[\mathcal{Q}, T_m] = mT_m$.
 292 For the spin ladder Hamiltonian we have $m \in \{0, \pm 2\}$. The operator T_m decomposes into a sum
 293 of local operators $\tau_{m,l}$ on a link l connecting different sites of the underlying lattice. When the
 294 above prerequisites are fulfilled the pCUT method unitarily transforms the original Hamilto-
 295 nian, order by order in the perturbation parameter λ , to an effective, quasiparticle-conserving
 296 Hamiltonian \mathcal{H}_{eff} reducing the complicated many-body problem to an easier effective few-body
 297 problem. The effective Hamiltonian in a generic form for an arbitrary number of expansion
 298 parameters λ_i is then given by

$$\mathcal{H}_{\text{eff}} = \mathcal{H}_0 + \sum_{\sum_j^{N_\lambda} n_j = k} \lambda_1^{n_1} \dots \lambda_{N_\lambda}^{n_{N_\lambda}} \sum_{\substack{\dim(\mathbf{m})=k, \\ \sum_i m_i = 0}} C(\mathbf{m}) T_{m_1} \dots T_{m_k} \quad (13)$$

299 where the coefficients $C(\mathbf{m})$ are exactly given by rational numbers and the condition $\sum_i m_i = 0$
 300 enforces the quasiparticle conservation $[\mathcal{Q}, \mathcal{H}_{\text{eff}}] = 0$. Analogously, an effective observable is
 301 given by

$$\mathcal{O}_{\text{eff}} = \sum_{\sum_j^{N_\lambda} n_j = k} \lambda_1^{n_1} \dots \lambda_{N_\lambda}^{n_{N_\lambda}} \sum_{i=1}^{k+1} \sum_{\dim(\mathbf{m})=k} \tilde{C}(\mathbf{m}; i) T_{m_1} \dots T_{m_{i-1}} \mathcal{O} T_{m_i} \dots T_{m_k} \quad (14)$$

302 with the rational coefficient $\tilde{C}(\mathbf{m}; i)$. In contrast to the effective Hamiltonian the effective
 303 observable is not quasiparticle conserving. The effective Hamiltonian and observables are
 304 generally independent of the exact form of the original Hamiltonian as long as the pCUT pre-
 305 requisites are satisfied. To bring \mathcal{H}_{eff} and \mathcal{O}_{eff} into normal-ordered form, a model-dependent
 306 extraction process must be applied. For long-range interactions this is done most efficiently by
 307 a full-graph decomposition.

308 A.2 Graph decomposition

309 We apply the effective quantities to finite, topologically distinct graphs to bring them into
 310 normal-ordered structure. We refer to this approach as a linked-cluster expansion imple-
 311 mented as a full-graph decomposition. The underlying principle is the linked-cluster theo-
 312 rem which states that only linked processes have an overall contributions to cluster-additive
 313 quantities [89]. Since the effective pCUT Hamiltonian and observables are cluster-additive
 314 quantities we can reformulate Eqs. (13) and (14) as

$$\mathcal{H}_{\text{eff}} = \mathcal{H}_0 + \sum_{\sum_j^{N_\lambda} n_j = k} \lambda_1^{n_1} \dots \lambda_{N_\lambda}^{n_{N_\lambda}} \sum_{\substack{\dim(\mathbf{m})=k, \\ \sum_i m_i = 0}} \sum_{\substack{\mathcal{G}, \\ |\mathcal{E}_{\mathcal{G}}| \leq k}} C(\mathbf{m}) \sum_{\substack{l_1, \dots, l_k, \\ \bigcup_{i=1}^k l_i = \mathcal{G}}} \tau_{m_1, l_1} \dots \tau_{m_k, l_k}, \quad (15)$$

$$\mathcal{O}_{\text{eff}} = \sum_{\sum_j^{N_\lambda} n_j = k} \lambda_1^{n_1} \dots \lambda_{N_\lambda}^{n_{N_\lambda}} \sum_{i=1}^{k+1} \sum_{\dim(\mathbf{m})=k} \sum_{\substack{\mathcal{G}, \\ |\mathcal{E}_{\mathcal{G}}| \leq k}} \tilde{C}(\mathbf{m}; i) \sum_{\substack{l_1, \dots, l_k, \\ \bigcup_{i=1}^k l_i \cup x = \mathcal{G}}} \tau_{m_1, l_1} \dots \tau_{m_{i-1}, l_{i-1}} \mathcal{O}_x \tau_{m_i, l_i} \dots \tau_{m_k, l_k}, \quad (16)$$

315 where the sum over \mathcal{G} runs over all possible simple connected graphs of perturbative order
 316 $k \geq |\mathcal{E}_{\mathcal{G}}|$. A graph \mathcal{G} is a tuple $(\mathcal{E}_{\mathcal{G}}, \mathcal{V}_{\mathcal{G}})$ consisting of an edge or link set $\mathcal{E}_{\mathcal{G}}$ with $|\mathcal{E}_{\mathcal{G}}|$ edges and
 317 a set of vertices or sites $\mathcal{V}_{\mathcal{G}}$ with $|\mathcal{V}_{\mathcal{G}}|$ vertices. The conditions $\bigcup_{i=1}^k l_i = \mathcal{G}$ and $\bigcup_{i=1}^k l_i \cup x = \mathcal{G}$
 318 arising from the linked-cluster theorem ensure that the cluster made up of active links and
 319 sites during a process must match with the edge and vertex set of a simple connected graph
 320 \mathcal{G} . Note, we generalized the notation for observables \mathcal{O}_x where the index x can either refer
 321 to a site (local observable) or a link (non-local observable). Thus, we can set up a full-graph
 322 decomposition applying the effective quantities to a set of finite, topologically distinct, simple
 323 connected graphs.

324 In the standard approach one would identify different expansion parameters with link colors
 325 which serve as another topological attribute in the classification of graphs. However, this
 326 approach fails for long-range interactions because every coupling parameter $\lambda(\delta)$ between
 327 sites of distance δ would be associated to a distinct link color and the number of graphs would
 328 already be infinite in first order of perturbation. We can overcome this obstacle by introducing
 329 white graphs [89] where different link colors are ignored in the topological classification of
 330 graphs and instead additional information is tracked during the calculation on white graphs. In
 331 particular, every link on a graph is associated with a distinct expansion parameter $\lambda_n^{\mathcal{G}}$ yielding
 332 a multivariable polynomial after applying the effective quantities to the graph. Only during
 333 the embedding on the lattice the proper link color is reintroduced by replacing the expansion
 334 parameters of the polynomial by the actual coupling strength for each realization decaying
 335 algebraically with the distance between interacting sites.

336 A.3 Monte Carlo embedding

337 Since we describe the ladder system in the language of rung dimers as super sites the graph
 338 contributions from the linked-cluster expansion must be embedded into a one-dimensional
 339 chain to determine the values of physical quantities $\kappa = \sum_m c_m^{(\kappa)} \lambda^m$ as a high-order series in
 340 the thermodynamic limit. Due to the infinite range of the algebraically decaying interactions
 341 every graph can be embedded infinitely many times at any order of perturbation. For each real-
 342 ization of a graph on the infinite chain the generic couplings $\lambda_n^{\mathcal{G}}$ in the multivariable polynomial
 343 corresponding to distinct edges is substituted by the true coupling strength $\lambda(-1)^{\delta} |\delta|^{-1-\sigma}$ or
 344 $\lambda(-1)^{1+\delta} |1 + \delta|^{-1-\sigma}$ between graph vertices on sites i and $i + \delta$ on the chain. For a prefactor
 345 c_m in the high-order series only (reduced) contributions from graphs with up to m links and
 346 $m + 1$ sites can contribute. See Ref. [89] for remarks about reduced quantities. We can write
 347 explicitly

$$c_m^{(\kappa)} = \sum_{N=2}^{m+1} \sum_a f_N(a) = \sum_{N=2}^{m+1} S[f_N], \quad (17)$$

348 where the first sum goes over the number of vertices and the second sum over all possible
 349 configurations excluding embeddings with overlapping vertices. The integrand f_N combines all
 350 contributions from graphs with the same number of vertices N since the $m - 1$ sums contained
 351 in the sum \sum_a are identical for graphs with the same number of vertices. The integration of
 352 these high-dimensional infinite nested sums $S[\cdot]$ quickly becomes very challenging when the
 353 perturbative order increases. It is essential to use Monte Carlo (MC) integration to evaluate
 354 these sums since MC techniques are known to be well suited for high-dimensional problems.
 355 We take a Markov-chain Monte Carlo approach to sample the configuration space [57]. The
 356 fundamental moves consist of randomly selecting and moving graph vertices on the chain. For
 357 every embedding the integrands f_N are evaluated with the correct couplings and added up to
 358 the overall contributions [57].

359 A.4 Derivation of physical quantities

360 After having established the theoretical framework of the pCUT approach, we derive the phys-
 361 ical quantities used in this communication. We start by stating the normal-ordered effective
 362 one-triplon (1QP) Hamiltonian given by

$$\mathcal{H}_{\text{eff}}^{1\text{QP}} = \bar{E}_0 + \sum_{\rho} \sum_{j, \delta \geq 0} a_{\delta} (t_{j, \rho}^{\dagger} t_{j+\delta, \rho} + \text{h.c.}) \quad (18)$$

363 with the ground-state energy \bar{E}_0 and the 1QP hopping amplitudes a_{δ} . We determine the
 364 ground-state energy

$$\bar{E}_0 = \sum_m c_m^{(\bar{E}_0)} \lambda^m \quad (19)$$

365 in the thermodynamic limit as a high-order series in the perturbation parameter λ using the
 366 above described procedure where the general white-graph contributions must be embedded
 367 into the infinite chain of dimer supersites using Monte Carlo summation yielding estimates for
 368 $c_m^{(\bar{E}_0)}$. The control parameter susceptibility can be directly obtained using

$$\chi = \frac{d^2 \bar{E}_0}{d\lambda^2}. \quad (20)$$

369 To get the one-triplon excitation gap as a high-order series, we remember that Eq. (18) can be
 370 diagonalized by transforming into momentum space, yielding

$$\tilde{\mathcal{H}}_{\text{eff}}^{1\text{QP}} = \bar{E}_0 + \sum_{k, \rho} \omega(k) t_{k, \rho}^{\dagger} t_{k, \rho} \quad \text{with} \quad \omega(k) = a_0 + 2 \sum_{\delta > 0} a_{\delta} \cos(k\delta), \quad (21)$$

371 so the one-triplon gap is given by

$$\Delta = \min_k \omega(k) = \omega(k_c) = \sum_m c_m^{(\Delta)} \lambda^m \quad (22)$$

372 with the critical momentum $k_c = \pi$ for antiferromagnetic interactions. Analogously to the
 373 ground-state energy, we determine Monte Carlo estimates for $c_m^{(\Delta)}$. Last, we introduce the
 374 dynamic structure factor

$$S_{\rho, \rho}(k, \omega) = \frac{1}{2\pi N} \sum_{i, j} \int_{-\infty}^{\infty} dt \exp\{i[\omega t - k(j-i)]\} \langle \mathcal{O}_{i, \rho}(t) \mathcal{O}_{j, \rho}(0) \rangle, \quad (23)$$

375 with the observable defined as the antisymmetric combination of spin operators

$$\mathcal{O}_{i, \rho} = \frac{1}{2} (S_{i,1}^{\rho} - S_{i,2}^{\rho}) = \frac{1}{2} (t_{i, \rho}^{\dagger} + t_{i, \rho}) \quad (24)$$

376 of flavor ρ on a rung i . We now follow the steps in Ref. [97]. Integrating out the energy ω ,
 377 one can express the structure factor in the effective basis as a sum over spectral weights $S_{\rho, \rho}^{n\text{QP}}$
 378 with fixed quasi-particle number

$$S_{\rho, \rho}(k) = \sum_n S_{\rho, \rho}^{n\text{QP}}(k). \quad (25)$$

379 By changing into the Heisenberg picture we eventually arrive at

$$S_{\rho, \rho}^{1\text{QP}}(k) = \left| \langle t_{k, \rho} | \mathcal{O}_{\text{eff}, \rho}^{1\text{QP}}(k) | \text{ref} \rangle \right|^2 = |s(k)|^2 \quad (26)$$

380 for the one-triplon spectral weight, where $|\text{ref}\rangle = \otimes_i |s_i\rangle$ is the unperturbed rung-singlet
 381 ground state and $|t_{k,\rho}\rangle$ is the one-triplon state with momentum k and flavor ρ . In second
 382 quantization the effective observable restricted to the one-triplon channel can be expressed as
 383

$$\mathcal{O}_{\text{eff},\rho}^{1\text{QP}}(k) = s(k)(t_{k,\rho}^\dagger + t_{k,\rho}). \quad (27)$$

384 Due to the SU(2)-symmetry one has $\mathcal{S}_{x,x} = \mathcal{S}_{y,y} = \mathcal{S}_{z,z}$, we restrict in the following to $\rho = z$
 385 and calculate $S^{1\text{QP}} \equiv \mathcal{S}_{z,z}^{1\text{QP}}$. When we fix $k = k_c$ we can obtain a high order series of

$$s(k_c) = \sum_m c_m^{(s(k_c))} \lambda^m \quad (28)$$

386 from the Monte Carlo estimates of $c_m^{(s(k_c))}$ and determine one-triplon spectral weight simply by
 387 calculating the absolute square.

388 B DlogPadé extrapolations

389 To extract the quantum-critical point including critical exponents from the pCUT method well
 390 beyond the radius of convergence of the pure high-order series we use DlogPadé extrapola-
 391 tions. For a detailed description on DlogPadés and its application to critical phenomena we
 392 refer to Refs. [98, 99]. The Padé extrapolant of a physical quantity κ given as a perturbative
 393 series is defined as

$$P[L, M]_\kappa = \frac{P_L(\lambda)}{Q_M(\lambda)} = \frac{p_0 + p_1\lambda + \dots + p_L\lambda^L}{1 + q_1\lambda + \dots + q_M\lambda^M} \quad (29)$$

394 with $p_i, q_i \in \mathbb{R}$ and the degrees L, M of $P_L(x)$ and $Q_M(x)$ with $r \equiv L + M$, i.e., the Taylor
 395 expansion of Eq. (29) about $\lambda = 0$ up to order r must recover the quantity κ up to the same
 396 order. For DlogPadé extrapolants we introduce

$$\mathcal{D}(\lambda) = \frac{d}{d\lambda} \ln(\kappa) \equiv P[L, M]_{\mathcal{D}} \quad (30)$$

397 the Padé extrapolant of the logarithmic derivative \mathcal{D} with $r - 1 = L + M$. Thus the DlogPadé
 398 extrapolant of κ is given by

$$dP[L, M]_\kappa = \exp\left(\int_0^\lambda P[L, M]_{\mathcal{D}} d\lambda'\right). \quad (31)$$

399 Given a dominant power-law behavior $\kappa \sim |\lambda - \lambda_c|^{-\theta}$, an estimate for the critical point λ_c can
 400 be determined by excluding spurious extrapolants and analyzing the physical pole of $P[L, M]_{\mathcal{D}}$.
 401 If λ_c is known, we can define biased DlogPadés by the Padé extrapolant

$$\theta^* = (\lambda_c - \lambda) \frac{d}{d\lambda} \ln(\kappa) \equiv P[L, M]_{\theta^*} \quad (32)$$

402 In the unbiased as well as the biased case we can extract estimates for the critical exponent θ
 403 by calculating the residua

$$\begin{aligned} \theta_{\text{unbiased}} &= \text{Res } P[L, M]_{\mathcal{D}}|_{\lambda=\lambda_c}, \\ \theta_{\text{biased}} &= \text{Res } P[L, M]_{\theta^*}|_{\lambda=\lambda_c}. \end{aligned} \quad (33)$$

404 At the upper critical dimension $\sigma = 2/3$ multiplicative logarithmic corrections to the dominant
 405 power law behavior

$$\kappa \sim |\lambda - \lambda_c|^{-\theta} (\ln(\lambda - \lambda_c))^{p_\theta} \quad (34)$$

Table 1: Multiplicative logarithmic corrections p_θ at the upper critical dimension $\sigma_{uc} = 2/3$ associated to the ground-state energy p_α , the 1QP excitation gap $p_{z\nu}$, and the 1QP spectral weight $p_{(2-z-\eta)\nu}$. Expected values from field-theoretical consideration are read of from Refs. [100, 101].

	Multiplicative correction		
	P_α	$P_{z\nu}$	$P_{(2-z-\eta)\nu}$
Field-theoretical predictions	$\frac{1}{11} \approx 0.091$	$-\frac{5}{22} \approx -0.227$?
\mathcal{H}_\parallel	0.453(6)	-0.309(13)	3.94(11)
$\mathcal{H}_{\triangleright\triangleleft}$	0.533(16)	-0.374(19)	3.77(12)

406 in the vicinity of the quantum-critical point λ_c are present. By biasing the critical point λ_c and
407 the exponent θ to its mean-field value, we define

$$p_\theta^* = -\ln(1 - \lambda/\lambda_c)[(\lambda_c - \lambda)\mathcal{D}(\lambda) - \theta] \equiv P[L, M]_{p_\theta^*}, \quad (35)$$

408 such that we can determine an estimate for p_θ by again calculating the residuum of the Padé ex-
409 trapolants $P[L, M]_{p_\theta^*}$. Note, for all quantities we calculate a large set of DlogPadé extrapolants
410 with $L + M = r' \leq r$, exclude defective extrapolants, and arrange the remaining DlogPadés in
411 families with $L - M = \text{const}$. Although individual extrapolations deviate from each other, the
412 quality of the extrapolations increases with the order of perturbation as members of different
413 families but mutual order r' converge. To systematically analyze the quantum-critical regime,
414 we take the mean of the highest order extrapolants of different families with more than one
415 member. Here, we use DlogPadé extrapolation for the gap series to determine the critical point
416 λ_c and the critical exponent $z\nu$. We then apply biased DlogPadé extrapolation with λ_c from
417 the one-tripolon gap to obtain estimates for α and $2 - z - \eta$ via the series of the susceptibility
418 and the one-tripolon spectral weight.

419 Multiplicative logarithmic exponents to the power law scaling for both ladder models \mathcal{H}_\parallel
420 and $\mathcal{H}_{\triangleright\triangleleft}$ can be found in Table 1. We find estimates in the correct order of magnitude for p_α
421 and $p_{z\nu}$ with better estimates for the logarithmic correction exponent of the gap. For $p_{(2-z-\eta)}$
422 there are no field-theoretical predictions directly available. Note, it is extremely challenging to
423 accurately extract logarithmic corrections since the extracted values are very sensitive on the
424 position of the critical point and DlogPadés are known to overestimate the critical value [38].

425 C Linear spin-wave calculations

426 We supplement the critical behavior determined by the pCUT approach with critical points
427 from linear spin-wave approximation. As spin-wave theory considers fluctuations about the
428 classical ground state it is certainly valid in the Néel-ordered phase of the long-range Heisen-
429 berg ladders. We start by mapping the spin operators to boson creation and annihilation opera-
430 tors using the Holstein-Primakoff transformation up to linear order in the boson operators. For
431 the antiferromagnetic Heisenberg spin ladder the system must be divided into two sublattices
432 constituting the expected antiferromagnetic Néel order for strong long-range interactions. The
433 transformation thus reads

$$\begin{aligned}
S_{i,1}^z &= S - a_{i,1}^\dagger a_{i,1} & S_{i,1}^- &\approx \sqrt{2S} a_{i,1}^\dagger & S_{i,1}^+ &\approx \sqrt{2S} a_{i,1}, \\
S_{i,2}^z &= b_{i,2}^\dagger b_{i,2} - S & S_{i,2}^- &\approx \sqrt{2S} b_{i,2} & S_{i,2}^+ &\approx \sqrt{2S} b_{i,2}^\dagger, \\
S_{j,1}^z &= b_{j,1}^\dagger b_{j,1} - S & S_{j,1}^- &\approx \sqrt{2S} b_{j,1} & S_{j,1}^+ &\approx \sqrt{2S} b_{j,1}^\dagger, \\
S_{j,2}^z &= S - a_{j,2}^\dagger a_{j,2} & S_{j,2}^- &\approx \sqrt{2S} a_{j,2}^\dagger & S_{j,2}^+ &\approx \sqrt{2S} a_{j,2}
\end{aligned} \quad (36)$$

434 with i odd and j even rungs. Inserting these identities into the Hamiltonian \mathcal{H}_{\parallel} , neglecting
435 quartic terms and Fourier transforming the problem we arrive at

$$\begin{aligned} \mathcal{H}_{\parallel}^{\text{SW}} \approx \text{const.} + S \sum_k \left\{ \sum_{\nu} \left[(\gamma - f(k)) (a_{k,\nu}^{\dagger} a_{k,\nu} + b_{-k,\nu}^{\dagger} b_{-k,\nu}) + g(k) (a_{k,\nu} b_{-k,\nu} + a_{k,\nu}^{\dagger} b_{-k,\nu}^{\dagger}) \right] \right. \\ \left. + a_{k,1} b_{-k,2} + a_{k,2} b_{-k,1} + a_{k,1}^{\dagger} b_{-k,2}^{\dagger} + a_{k,2}^{\dagger} b_{-k,1}^{\dagger} \right\}. \end{aligned} \quad (37)$$

436 Incorporating the long-range couplings for an infinite chain into the prefactors we can define
437 the quantities

$$\begin{aligned} \gamma &= 1 + 2\lambda \sum_{\delta=1}^{\infty} \frac{1}{(2\delta-1)^{1+\sigma}}, \\ f(k) &= 2\lambda \sum_{\delta=1}^{\infty} \frac{\cos(2k\delta) - 1}{(2\delta)^{1+\sigma}}, \\ g(k) &= 2\lambda \sum_{\delta=1}^{\infty} \frac{\cos[(2\delta-1)k]}{(2\delta-1)^{1+\sigma}}. \end{aligned} \quad (38)$$

438 This Hamiltonian is quadratic in creation and annihilation operators in quasimomenta and we
439 intend to diagonalize the problem employing a Bogoliubov-Valatin transformation. Following
440 Ref. [102] we introduce the operator

$$\vec{\psi}_k^{\dagger} = (\vec{c}_k^{\dagger} \quad \vec{c}_k^T) = (a_{k,1}^{\dagger} \quad b_{-k,1}^{\dagger} \quad a_{k,2}^{\dagger} \quad b_{-k,2}^{\dagger} \quad a_{k,1} \quad b_{-k,1} \quad a_{k,2} \quad b_{-k,2}). \quad (39)$$

441 We use this operator to bring the spin-wave Hamiltonian into canonical quadratic form

$$\mathcal{H}_{\parallel}^{\text{SW}} = \sum_k \left[\frac{1}{2} \vec{\psi}_k^{\dagger} \underbrace{\begin{pmatrix} A_k & B_k \\ B_k^{\dagger} & A_k^T \end{pmatrix}}_{\equiv M_k} \vec{\psi}_k - \frac{1}{2} \text{tr} A_k \right], \quad (40)$$

442 where A_k and M_k are Hermitian matrices and B_k is a symmetric matrix. To solve the diag-
443 onalization problem we must find a transformation $\vec{\psi}_k = T \vec{\varphi}_k$ that brings M_k into diagonal
444 form and preserves the bosonic anticommutation relations of $\vec{\psi}_k$. Xiao [102] proofs that the
445 problem can be reformulated in terms of the eigenvalue problem of the dynamic matrix

$$D_k = \begin{pmatrix} A_k & B_k \\ -B_k^{\dagger} & -A_k^T \end{pmatrix} \quad (41)$$

446 arising from the Heisenberg equation of motion and that the transformation matrix T can
447 be constructed using appropriately normalized eigenvectors. A physical solution to the prob-
448 lem exists if and only if the dynamical matrix is diagonalizable and the eigenvalues are real.
449 Employing this scheme we find

$$\mathcal{H}_{\parallel}^{\text{SW}} = \text{const.} + S \sum_{k,\nu} \left(\omega_+(k) \alpha_{k,\nu}^{\dagger} \alpha_{k,\nu} + \omega_-(k) \beta_{k,\nu}^{\dagger} \beta_{k,\nu} \right) \quad (42)$$

450 in terms of the new boson creation and annihilation operators $\alpha_{k,\nu}^{(\dagger)}$ and $\beta_{k,\nu}^{(\dagger)}$ and the spin-wave
451 dispersion

$$\omega_{\pm}(k) = \sqrt{(\gamma - f(k))^2 - (g(k) \pm 1)^2}. \quad (43)$$

452 In the limit $\lambda \rightarrow \infty$ we recover the spin-wave dispersion in Ref. [41] for the long-range Heisen-
453 berg spin chain. The staggered magnetization deep in the antiferromagnetic regime can be

454 expressed as $m = S - \Delta m$ where Δm is the correction induced by quantum fluctuations. We
 455 start with the expression

$$\Delta m = \sum_{\nu=1}^2 \langle a_{j,\nu}^\dagger a_{j,\nu} \rangle \stackrel{N \rightarrow \infty}{=} \frac{1}{\pi} \sum_{\nu} \int_{-\pi/2}^{\pi/2} dk \langle a_{k,\nu}^\dagger a_{k,\nu} \rangle \quad (44)$$

456 and rewriting it in terms of the boson operators $\alpha_{k,\nu}^{(\dagger)}$ and $\beta_{k,\nu}^{(\dagger)}$ we find

$$\Delta m = \frac{1}{\pi} \int_{-\pi/2}^{\pi/2} dk \left[\frac{1}{2} \left(\frac{\gamma - f(k)}{\omega_+(k)} + \frac{\gamma - f(k)}{\omega_-(k)} \right) - 1 \right]. \quad (45)$$

457 Introducing the linear Holstein-Primakoff transformation for the Hamiltonian $\mathcal{H}_{\triangleright\triangleleft}$ including
 458 diagonal long-range interactions the linear spin-wave Hamiltonian reads

$$\begin{aligned} \mathcal{H}_{\triangleright\triangleleft}^{SW} = \text{const.} + S \sum_k \{ & \sum_{\nu} [(\Gamma - f(k)) (a_{k,\nu}^\dagger a_{k,\nu} + b_{-k,\nu}^\dagger b_{-k,\nu}) + g(k) (a_{k,\nu} b_{-k,\nu} + a_{k,\nu}^\dagger b_{-k,\nu}^\dagger)] \\ & + v(k) (a_{k,1} b_{-k,2} + a_{k,2} b_{-k,1} + a_{k,1}^\dagger b_{-k,2}^\dagger + a_{k,2}^\dagger b_{-k,1}^\dagger) \\ & + w(k) (a_{k,1}^\dagger a_{k,2} + a_{k,2}^\dagger a_{k,1} + b_{-k,1}^\dagger b_{-k,2} + b_{-k,2}^\dagger b_{-k,1}) \}, \end{aligned} \quad (46)$$

459 where we introduced the multiple prefactors defined as $\kappa = \kappa_1 + \kappa_2$, $\Gamma = \gamma + \kappa$ and as

$$\begin{aligned} \kappa_1 &= 2\lambda \sum_{\delta=1}^{\infty} \frac{1}{((2\delta)^2 + 1)^{\frac{1+\sigma}{2}}}, \\ \kappa_2 &= 2\lambda \sum_{\delta=1}^{\infty} \frac{1}{((2\delta - 1)^2 + 1)^{\frac{1+\sigma}{2}}}, \\ v(k) &= 1 + 2\lambda \sum_{\delta=1}^{\infty} \frac{\cos(2\delta k)}{((2\delta)^2 + 1)^{\frac{1+\sigma}{2}}}, \\ w(k) &= 2\lambda \sum_{\delta=1}^{\infty} \frac{\cos[(2\delta - 1)k]}{((2\delta - 1)^2 + 1)^{\frac{1+\sigma}{2}}}. \end{aligned} \quad (47)$$

460 Again employing the same Bogoliubov-Valatin transformation we can derive the spin-wave
 461 dispersion

$$\omega_{\pm}(k) = \sqrt{[\Gamma - (f(k) \pm w(k))]^2 - [g(k) \pm v(k)]^2} \quad (48)$$

462 and the corrections to the staggered magnetization

$$\Delta m = \frac{1}{\pi} \int_{-\pi/2}^{\pi/2} dk \left[\frac{1}{2} \left(\frac{\Gamma - f(k) - w(k)}{\omega_+(k)} + \frac{\Gamma - f(k) + w(k)}{\omega_-(k)} \right) - 1 \right]. \quad (49)$$

463 For both Hamiltonians \mathcal{H}_{\parallel} and $\mathcal{H}_{\triangleright\triangleleft}$ we evaluate the integrals Δm numerically and use the
 464 consistency condition $\Delta m < S$ in the antiferromagnetic regime to approximate the quantum
 465 phase transition line.

466 D (Hyper-) scaling relations

467 In renormalization group (RG) theory the generalized homogeneity of the free energy density
 468 is exploited [103]. Connecting the critical exponents of observables with the derivatives of the

469 free energy density and exploiting the homogeneity properties, the (hyper-) scaling relations

$$\gamma = (2 - \eta) \nu, \quad (\text{Fisher equality}) \quad (50)$$

$$\gamma = \beta(\delta - 1), \quad (\text{Widom equality}) \quad (51)$$

$$2 = \alpha + 2\beta + \gamma, \quad (\text{Essam-Fisher equality}) \quad (52)$$

$$2 - \alpha = (d + z) \nu \text{ for } d \leq d_{\text{uc}}, \quad (\text{Hyperscaling relation}) \quad (53)$$

470 can be derived. However, the hyperscaling relation breaks down above the upper critical
471 dimension due to dangerous irrelevant variables in the free energy sector since these variables
472 cannot be set to zero as the free energy density becomes singular in this limit [104, 105].
473 Allowing the correlation sector to be affected by dangerous irrelevant variables for quantum
474 systems in analogy to previous works in classical systems [106, 107] the hyperscaling relation
475 can be generalized to

$$2 - \alpha = \left(\frac{d}{\varphi} + z \right) \nu \quad (54)$$

476 with the pseudocritical exponent $\varphi = \max(1, d/d_{\text{uc}})$ [39]. As the one-dimensional $O(3)$ quan-
477 tum rotor model can be mapped to the low-energy properties of the dimerized antiferromag-
478 netic Heisenberg ladder [90] we can use the long-range mean-field critical exponents

$$\gamma = 1, \quad \nu = \frac{1}{\sigma}, \quad z = \frac{\sigma}{2}, \quad \eta = 2 - \sigma \quad (55)$$

479 derived from one-loop RG [59] for the long-range $O(3)$ quantum rotor model at the upper
480 critical dimension and insert them into Eq. (52). We find $d_{\text{uc}}(\sigma) = 3\sigma/2$. It directly follows
481 that $d > d_{\text{uc}}$ in the regime $\sigma < 2/3$. Thus, we can rewrite

$$\varphi = \max\left(1, \frac{2}{3\sigma}\right) = \begin{cases} 1 & \text{for } \sigma \geq 2/3 \\ \frac{2}{3\sigma} & \text{for } \sigma < 2/3 \end{cases} \quad (56)$$

482 which together with Eq. (54) is the generalized hyperscaling relation as derived in Ref. [39].

483 References

- 484 [1] D. Bitko, T. F. Rosenbaum and G. Aeppli, *Quantum critical behavior for a model magnet*,
485 Phys. Rev. Lett. **77**, 940 (1996), doi:[10.1103/PhysRevLett.77.940](https://doi.org/10.1103/PhysRevLett.77.940).
- 486 [2] P. B. Chakraborty, P. Henelius, H. Kjønsberg, A. W. Sandvik and S. M. Girvin, "", Phys.
487 Rev. B **70**, 144411 (2004), doi:[10.1103/PhysRevB.70.144411](https://doi.org/10.1103/PhysRevB.70.144411).
- 488 [3] S. T. Bramwell and M. J. P. Gingras, *Spin ice state in frustrated magnetic pyrochlore*
489 *materials*, Science **294**(5546), 1495 (2001), doi:[10.1126/science.1064761](https://doi.org/10.1126/science.1064761).
- 490 [4] C. Castelnovo, R. Moessner and S. L. Sondhi, *Magnetic monopoles in spin ice*, Nature
491 **452**(7175), 43 (2008), doi:[10.1038/nature06433](https://doi.org/10.1038/nature06433).
- 492 [5] R. Islam, E. E. Edwards, K. Kim, S. Korenblit, C. Noh, H. Carmichael, G.-D. Lin, L.-M.
493 Duan, C.-C. Joseph Wang, J. K. Freericks and C. Monroe, *Onset of a quantum phase*
494 *transition with a trapped ion quantum simulator*, Nature Communications **2**(1), 377
495 (2011), doi:[10.1038/ncomms1374](https://doi.org/10.1038/ncomms1374).
- 496 [6] J. W. Britton, B. C. Sawyer, A. C. Keith, C.-C. J. Wang, J. K. Freericks, H. Uys,
497 M. J. Biercuk and J. J. Bollinger, *Engineered two-dimensional ising interactions in a*
498 *trapped-ion quantum simulator with hundreds of spins*, Nature **484**(7395), 489 (2012),
499 doi:[10.1038/nature10981](https://doi.org/10.1038/nature10981).

- 500 [7] R. Islam, C. Senko, W. C. Campbell, S. Korenblit, J. Smith, A. Lee, E. E. Edwards, C.-
501 C. J. Wang, J. K. Freericks and C. Monroe, *Emergence and frustration of magnetism with*
502 *variable-range interactions in a quantum simulator*, Science **340**(6132), 583 (2013),
503 doi:[10.1126/science.1232296](https://doi.org/10.1126/science.1232296).
- 504 [8] P. Jurcevic, B. P. Lanyon, P. Hauke, C. Hempel, P. Zoller, R. Blatt and C. F. Roos, *Quasipar-*
505 *ticle engineering and entanglement propagation in a quantum many-body system*, Nature
506 **511**(7508), 202 (2014), doi:[10.1038/nature13461](https://doi.org/10.1038/nature13461).
- 507 [9] P. Richerme, Z.-X. Gong, A. Lee, C. Senko, J. Smith, M. Foss-Feig, S. Michalakis, A. V.
508 Gorshkov and C. Monroe, *Non-local propagation of correlations in quantum systems with*
509 *long-range interactions*, Nature **511**(7508), 198 (2014), doi:[10.1038/nature13450](https://doi.org/10.1038/nature13450).
- 510 [10] M. Mielenz, H. Kalis, M. Wittmer, F. Hakeberg, U. Warring, R. Schmied, M. Blain,
511 P. Maunz, D. L. Moehring, D. Leibfried and T. Schaetz, *Arrays of individually controlled*
512 *ions suitable for two-dimensional quantum simulations*, Nature Communications **7**(1),
513 ncomms11839 (2016), doi:[10.1038/ncomms11839](https://doi.org/10.1038/ncomms11839).
- 514 [11] J. G. Bohnet, B. C. Sawyer, J. W. Britton, M. L. Wall, A. M. Rey, M. Foss-Feig and J. J.
515 Bollinger, *Quantum spin dynamics and entanglement generation with hundreds of trapped*
516 *ions*, Science **352**(6291), 1297 (2016), doi:[10.1126/science.aad9958](https://doi.org/10.1126/science.aad9958).
- 517 [12] P. Jurcevic, H. Shen, P. Hauke, C. Maier, T. Brydges, C. Hempel, B. P. Lanyon, M. Heyl,
518 R. Blatt and C. F. Roos, *Direct observation of dynamical quantum phase transi-*
519 *tions in an interacting many-body system*, Phys. Rev. Lett. **119**, 080501 (2017),
520 doi:[10.1103/PhysRevLett.119.080501](https://doi.org/10.1103/PhysRevLett.119.080501).
- 521 [13] J. Zhang, G. Pagano, P. W. Hess, A. Kyprianidis, P. Becker, H. Kaplan, A. V. Gorshkov, Z.-X.
522 Gong and C. Monroe, *Observation of a many-body dynamical phase transition with a 53-*
523 *qubit quantum simulator*, Nature **551**(7682), 601 (2017), doi:[10.1038/nature24654](https://doi.org/10.1038/nature24654).
- 524 [14] B. Žunkovič, M. Heyl, M. Knap and A. Silva, *Dynamical quantum phase transitions*
525 *in spin chains with long-range interactions: Merging different concepts of nonequilibrium*
526 *criticality*, Phys. Rev. Lett. **120**, 130601 (2018), doi:[10.1103/PhysRevLett.120.130601](https://doi.org/10.1103/PhysRevLett.120.130601).
- 527 [15] C. Hempel, C. Maier, J. Romero, J. McClean, T. Monz, H. Shen, P. Jurcevic, B. P.
528 Lanyon, P. Love, R. Babbush, A. Aspuru-Guzik, R. Blatt *et al.*, *Quantum chemistry*
529 *calculations on a trapped-ion quantum simulator*, Phys. Rev. X **8**, 031022 (2018),
530 doi:[10.1103/PhysRevX.8.031022](https://doi.org/10.1103/PhysRevX.8.031022).
- 531 [16] M. K. Joshi, F. Kranzl, A. Schuckert, I. Lovas, C. Maier, R. Blatt, M. Knap and C. F.
532 Roos, *Observing emergent hydrodynamics in a long-range quantum magnet*, Science
533 **376**(6594), 720 (2022), doi:[10.1126/science.abk2400](https://doi.org/10.1126/science.abk2400).
- 534 [17] H. Weimer, M. Müller, I. Lesanovsky, P. Zoller and H. P. Büchler, *A rydberg quantum*
535 *simulator*, Nature Physics **6**(5), 382 (2010), doi:[10.1038/nphys1614](https://doi.org/10.1038/nphys1614).
- 536 [18] T. Xia, M. Lichtman, K. Maller, A. W. Carr, M. J. Piotrowicz, L. Isenhower and M. Saffman,
537 *Randomized benchmarking of single-qubit gates in a 2d array of neutral-atom qubits*, Phys.
538 Rev. Lett. **114**, 100503 (2015), doi:[10.1103/PhysRevLett.114.100503](https://doi.org/10.1103/PhysRevLett.114.100503).
- 539 [19] H. Labuhn, D. Barredo, S. Ravets, S. de Léséleuc, T. Macrì, T. Lahaye and A. Browaeys,
540 *Tunable two-dimensional arrays of single rydberg atoms for realizing quantum ising mod-*
541 *els*, Nature **534**(7609), 667 (2016), doi:[10.1038/nature18274](https://doi.org/10.1038/nature18274).

- 542 [20] Y. Wang, A. Kumar, T.-Y. Wu and D. S. Weiss, *Single-qubit gates based on tar-*
543 *geted phase shifts in a 3d neutral atom array*, *Science* **352**(6293), 1562 (2016),
544 doi:[10.1126/science.aaf2581](https://doi.org/10.1126/science.aaf2581).
- 545 [21] P. Schauss, *Quantum simulation of transverse ising models with rydberg atoms*, *Quantum*
546 *Science and Technology* **3**(2), 023001 (2018), doi:[10.1088/2058-9565/aa9c59](https://doi.org/10.1088/2058-9565/aa9c59).
- 547 [22] S. de Léséleuc, V. Lienhard, P. Scholl, D. Barredo, S. Weber, N. Lang, H. P. Büch-
548 *ler*, T. Lahaye and A. Browaeys, *Observation of a symmetry-protected topological*
549 *phase of interacting bosons with rydberg atoms*, *Science* **365**(6455), 775 (2019),
550 doi:[10.1126/science.aav9105](https://doi.org/10.1126/science.aav9105).
- 551 [23] H. Levine, A. Keesling, G. Semeghini, A. Omran, T. T. Wang, S. Ebadi, H. Bernien,
552 M. Greiner, V. Vuletić, H. Pichler and M. D. Lukin, *Parallel implementation of high-*
553 *fidelity multiqubit gates with neutral atoms*, *Phys. Rev. Lett.* **123**, 170503 (2019),
554 doi:[10.1103/PhysRevLett.123.170503](https://doi.org/10.1103/PhysRevLett.123.170503).
- 555 [24] T.-Y. Wu, A. Kumar, F. Giraldo and D. S. Weiss, *Stern–gerlach detection of neutral-*
556 *atom qubits in a state-dependent optical lattice*, *Nature Physics* **15**(6), 538 (2019),
557 doi:[10.1038/s41567-019-0478-8](https://doi.org/10.1038/s41567-019-0478-8).
- 558 [25] S. Ebadi, T. T. Wang, H. Levine, A. Keesling, G. Semeghini, A. Omran, D. Bluvstein,
559 R. Samajdar, H. Pichler, W. W. Ho, S. Choi, S. Sachdev *et al.*, *Quantum phases of mat-*
560 *ter on a 256-atom programmable quantum simulator*, *Nature* **595**(7866), 227 (2021),
561 doi:[10.1038/s41586-021-03582-4](https://doi.org/10.1038/s41586-021-03582-4).
- 562 [26] G. Semeghini, H. Levine, A. Keesling, S. Ebadi, T. T. Wang, D. Bluvstein, R. Verresen,
563 H. Pichler, M. Kalinowski, R. Samajdar, A. Omran, S. Sachdev *et al.*, *Probing topological*
564 *spin liquids on a programmable quantum simulator*, *Science* **374**(6572), 1242 (2021),
565 doi:[10.1126/science.abi8794](https://doi.org/10.1126/science.abi8794).
- 566 [27] M. Saffman, T. G. Walker and K. Mølmer, *Quantum information with rydberg atoms*,
567 *Rev. Mod. Phys.* **82**, 2313 (2010), doi:[10.1103/RevModPhys.82.2313](https://doi.org/10.1103/RevModPhys.82.2313).
- 568 [28] C. D. Bruzewicz, J. Chiaverini, R. McConnell and J. M. Sage, *Trapped-ion quantum*
569 *computing: Progress and challenges*, *Applied Physics Reviews* **6**(2), 021314 (2019),
570 doi:[10.1063/1.5088164](https://doi.org/10.1063/1.5088164).
- 571 [29] A. Browaeys and T. Lahaye, *Many-body physics with individually controlled rydberg*
572 *atoms*, *Nature Physics* **16**(2), 132 (2020), doi:[10.1038/s41567-019-0733-z](https://doi.org/10.1038/s41567-019-0733-z).
- 573 [30] A. W. Sandvik, *Stochastic series expansion method for quantum ising models with arbitrary*
574 *interactions*, *Phys. Rev. E* **68**, 056701 (2003), doi:[10.1103/PhysRevE.68.056701](https://doi.org/10.1103/PhysRevE.68.056701).
- 575 [31] T. Koffel, M. Lewenstein and L. Tagliacozzo, *Entanglement Entropy for the Long-*
576 *Range Ising Chain in a Transverse Field*, *Phys. Rev. Lett.* **109**, 267203 (2012),
577 doi:[10.1103/PhysRevLett.109.267203](https://doi.org/10.1103/PhysRevLett.109.267203).
- 578 [32] M. Knap, A. Kantian, T. Giamarchi, I. Bloch, M. D. Lukin and E. Demler, *Probing Real-*
579 *Space and Time-Resolved Correlation Functions with Many-Body Ramsey Interferometry*,
580 *Phys. Rev. Lett.* **111**, 147205 (2013), doi:[10.1103/PhysRevLett.111.147205](https://doi.org/10.1103/PhysRevLett.111.147205).
- 581 [33] G. Sun, *Fidelity susceptibility study of quantum long-range antiferromagnetic ising chain*,
582 *Phys. Rev. A* **96**, 043621 (2017), doi:[10.1103/PhysRevA.96.043621](https://doi.org/10.1103/PhysRevA.96.043621).

- 583 [34] Z. Zhu, G. Sun, W.-L. You and D.-N. Shi, *Fidelity and criticality of a quan-*
584 *tum ising chain with long-range interactions*, Phys. Rev. A **98**, 023607 (2018),
585 doi:[10.1103/PhysRevA.98.023607](https://doi.org/10.1103/PhysRevA.98.023607).
- 586 [35] A. W. Sandvik, *Ground states of a frustrated quantum spin chain with long-range inter-*
587 *actions*, Phys. Rev. Lett. **104**, 137204 (2010), doi:[10.1103/PhysRevLett.104.137204](https://doi.org/10.1103/PhysRevLett.104.137204).
- 588 [36] L. Vanderstraeten, M. Van Damme, H. P. Büchler and F. Verstraete, *Quasiparticles in*
589 *quantum spin chains with long-range interactions*, Phys. Rev. Lett. **121**, 090603 (2018),
590 doi:[10.1103/PhysRevLett.121.090603](https://doi.org/10.1103/PhysRevLett.121.090603).
- 591 [37] S. Fey and K. P. Schmidt, *Critical behavior of quantum magnets with long-*
592 *range interactions in the thermodynamic limit*, Phys. Rev. B **94**, 075156 (2016),
593 doi:[10.1103/PhysRevB.94.075156](https://doi.org/10.1103/PhysRevB.94.075156).
- 594 [38] P. Adelhardt, J. A. Koziol, A. Schellenberger and K. P. Schmidt, *Quantum criticality and*
595 *excitations of a long-range anisotropic xy chain in a transverse field*, Phys. Rev. B **102**,
596 174424 (2020), doi:[10.1103/PhysRevB.102.174424](https://doi.org/10.1103/PhysRevB.102.174424).
- 597 [39] A. Langheld, J. A. Koziol, P. Adelhardt, S. C. Kapfer and K. P. Schmidt, *Scaling at quan-*
598 *tum phase transitions above the upper critical dimension*, SciPost Phys. **13**, 088 (2022),
599 doi:[10.21468/SciPostPhys.13.4.088](https://doi.org/10.21468/SciPostPhys.13.4.088).
- 600 [40] S. Yang, D.-X. Yao and A. W. Sandvik, *Deconfined quantum criticality in spin-1/2 chains*
601 *with long-range interactions*, doi:[10.48550/ARXIV.2001.02821](https://doi.org/10.48550/ARXIV.2001.02821) (2020).
- 602 [41] E. Yusuf, A. Joshi and K. Yang, *Spin waves in antiferromagnetic spin chains with long-*
603 *range interactions*, Phys. Rev. B **69**, 144412 (2004), doi:[10.1103/PhysRevB.69.144412](https://doi.org/10.1103/PhysRevB.69.144412).
- 604 [42] N. Laflorencie, I. Affleck and M. Berciu, *Critical phenomena and quantum phase*
605 *transition in long range heisenberg antiferromagnetic chains*, Journal of Statistical
606 Mechanics: Theory and Experiment **2005**(12), P12001 (2005), doi:[10.1088/1742-](https://doi.org/10.1088/1742-5468/2005/12/p12001)
607 [5468/2005/12/p12001](https://doi.org/10.1088/1742-5468/2005/12/p12001).
- 608 [43] R.-G. Zhu and A.-M. Wang, *Absence of long-range order in an antiferromagnetic chain*
609 *with long-range interactions: Green's function approach*, Phys. Rev. B **74**, 012406 (2006),
610 doi:[10.1103/PhysRevB.74.012406](https://doi.org/10.1103/PhysRevB.74.012406).
- 611 [44] Z.-H. Li and A.-M. Wang, *Matrix product state approach to a frustrated*
612 *spin chain with long-range interactions*, Phys. Rev. B **91**, 235110 (2015),
613 doi:[10.1103/PhysRevB.91.235110](https://doi.org/10.1103/PhysRevB.91.235110).
- 614 [45] Y. Tang and A. W. Sandvik, *Quantum monte carlo studies of spinons in one-dimensional*
615 *spin systems*, Phys. Rev. B **92**, 184425 (2015), doi:[10.1103/PhysRevB.92.184425](https://doi.org/10.1103/PhysRevB.92.184425).
- 616 [46] Z.-X. Gong, M. F. Maghrebi, A. Hu, M. Foss-Feig, P. Richerme, C. Monroe and A. V.
617 Gorshkov, *Kaleidoscope of quantum phases in a long-range interacting spin-1 chain*, Phys.
618 Rev. B **93**, 205115 (2016), doi:[10.1103/PhysRevB.93.205115](https://doi.org/10.1103/PhysRevB.93.205115).
- 619 [47] M. F. Maghrebi, Z.-X. Gong and A. V. Gorshkov, *Continuous symmetry breaking in*
620 *1d long-range interacting quantum systems*, Phys. Rev. Lett. **119**, 023001 (2017),
621 doi:[10.1103/PhysRevLett.119.023001](https://doi.org/10.1103/PhysRevLett.119.023001).
- 622 [48] J. Ren, W.-L. You and A. M. Oleś, *Quantum phase transitions in a spin-1 antiferromagnetic*
623 *chain with long-range interactions and modulated single-ion anisotropy*, Phys. Rev. B **102**,
624 024425 (2020), doi:[10.1103/PhysRevB.102.024425](https://doi.org/10.1103/PhysRevB.102.024425).

- 625 [49] D. Vodola, L. Lepori, E. Ercolessi, A. V. Gorshkov and G. Pupillo, *Ki-*
626 *taev chains with long-range pairing*, Phys. Rev. Lett. **113**, 156402 (2014),
627 doi:[10.1103/PhysRevLett.113.156402](https://doi.org/10.1103/PhysRevLett.113.156402).
- 628 [50] D. Vodola, L. Lepori, E. Ercolessi and G. Pupillo, *Long-range ising and kitaev models:*
629 *phases, correlations and edge modes*, New Journal of Physics **18**(1), 015001 (2015),
630 doi:[10.1088/1367-2630/18/1/015001](https://doi.org/10.1088/1367-2630/18/1/015001).
- 631 [51] S. Maity, U. Bhattacharya and A. Dutta, *One-dimensional quantum many body systems*
632 *with long-range interactions*, Journal of Physics A: Mathematical and Theoretical **53**(1),
633 013001 (2019), doi:[10.1088/1751-8121/ab5634](https://doi.org/10.1088/1751-8121/ab5634).
- 634 [52] D. Sadhukhan and J. Dziarmaga, *Is there a correlation length in a model with long-range*
635 *interactions?*, doi:[10.48550/ARXIV.2107.02508](https://doi.org/10.48550/ARXIV.2107.02508) (2021).
- 636 [53] R. Samajdar, W. W. Ho, H. Pichler, M. D. Lukin and S. Sachdev, *Quantum phases of*
637 *rydberg atoms on a kagome lattice*, Proceedings of the National Academy of Sciences
638 **118**(4), e2015785118 (2021), doi:[10.1073/pnas.2015785118](https://doi.org/10.1073/pnas.2015785118).
- 639 [54] R. Verresen, M. D. Lukin and A. Vishwanath, *Prediction of toric code*
640 *topological order from rydberg blockade*, Phys. Rev. X **11**, 031005 (2021),
641 doi:[10.1103/PhysRevX.11.031005](https://doi.org/10.1103/PhysRevX.11.031005).
- 642 [55] F. Liu, Z.-C. Yang, P. Bienias, T. Iadecola and A. V. Gorshkov, *Localization and criticality*
643 *in antiblockaded two-dimensional rydberg atom arrays*, Phys. Rev. Lett. **128**, 013603
644 (2022), doi:[10.1103/PhysRevLett.128.013603](https://doi.org/10.1103/PhysRevLett.128.013603).
- 645 [56] S. Humeniuk, *Quantum Monte Carlo study of long-range transverse-field*
646 *Ising models on the triangular lattice*, Phys. Rev. B **93**, 104412 (2016),
647 doi:[10.1103/PhysRevB.93.104412](https://doi.org/10.1103/PhysRevB.93.104412).
- 648 [57] S. Fey, S. C. Kapfer and K. P. Schmidt, *Quantum Criticality of Two-Dimensional Quan-*
649 *tum Magnets with Long-Range Interactions*, Phys. Rev. Lett. **122**, 017203 (2019),
650 doi:[10.1103/PhysRevLett.122.017203](https://doi.org/10.1103/PhysRevLett.122.017203).
- 651 [58] J. A. Koziol, A. Langheld, S. C. Kapfer and K. P. Schmidt, *Quantum-critical properties of*
652 *the long-range transverse-field ising model from quantum monte carlo simulations*, Phys.
653 Rev. B **103**, 245135 (2021), doi:[10.1103/PhysRevB.103.245135](https://doi.org/10.1103/PhysRevB.103.245135).
- 654 [59] A. Dutta and J. K. Bhattacharjee, *Phase transitions in the quantum Ising and*
655 *rotor models with a long-range interaction*, Phys. Rev. B **64**, 184106 (2001),
656 doi:[10.1103/PhysRevB.64.184106](https://doi.org/10.1103/PhysRevB.64.184106).
- 657 [60] J. Sak, *Recursion relations and fixed points for ferromagnets with long-range interactions*,
658 Phys. Rev. B **8**, 281 (1973), doi:[10.1103/PhysRevB.8.281](https://doi.org/10.1103/PhysRevB.8.281).
- 659 [61] N. Defenu, A. Trombettoni and S. Ruffo, *Criticality and phase diagram of quantum long-*
660 *range $o(n)$ models*, Phys. Rev. B **96**, 104432 (2017), doi:[10.1103/PhysRevB.96.104432](https://doi.org/10.1103/PhysRevB.96.104432).
- 661 [62] C. Behan, L. Rastelli, S. Rychkov and B. Zan, *Long-range critical expo-*
662 *nents near the short-range crossover*, Phys. Rev. Lett. **118**, 241601 (2017),
663 doi:[10.1103/PhysRevLett.118.241601](https://doi.org/10.1103/PhysRevLett.118.241601).
- 664 [63] C. Behan, L. Rastelli, S. Rychkov and B. Zan, *A scaling theory for the long-range*
665 *to short-range crossover and an infrared duality*, J. Phys. A **50**(35), 354002 (2017),
666 doi:[10.1088/1751-8121/aa8099](https://doi.org/10.1088/1751-8121/aa8099).

- 667 [64] N. Defenu, A. Codello, S. Ruffo and A. Trombettoni, *Criticality of spin systems with*
668 *weak long-range interactions*, J. Phys. A **53**(14), 143001 (2020), doi:[10.1088/1751-](https://doi.org/10.1088/1751-8121/ab6a6c)
669 [8121/ab6a6c](https://doi.org/10.1088/1751-8121/ab6a6c).
- 670 [65] L. Yang and A. E. Feiguin, *From deconfined spinons to coherent magnons in an antiferro-*
671 *magnetic Heisenberg chain with long range interactions*, SciPost Phys. **10**, 110 (2021),
672 doi:[10.21468/SciPostPhys.10.5.110](https://doi.org/10.21468/SciPostPhys.10.5.110).
- 673 [66] N. D. Mermin and H. Wagner, *Absence of ferromagnetism or antiferromagnetism in*
674 *one- or two-dimensional isotropic heisenberg models*, Phys. Rev. Lett. **17**, 1133 (1966),
675 doi:[10.1103/PhysRevLett.17.1133](https://doi.org/10.1103/PhysRevLett.17.1133).
- 676 [67] P. C. Hohenberg, *Existence of long-range order in one and two dimensions*, Phys. Rev.
677 **158**, 383 (1967), doi:[10.1103/PhysRev.158.383](https://doi.org/10.1103/PhysRev.158.383).
- 678 [68] S. Coleman, *There are no goldstone bosons in two dimensions*, Communications in
679 Mathematical Physics **31**(4), 259 (1973), doi:[10.1007/BF01646487](https://doi.org/10.1007/BF01646487).
- 680 [69] L. Pitaevskii and S. Stringari, *Uncertainty principle, quantum fluctuations, and*
681 *broken symmetries*, Journal of Low Temperature Physics **85**(5), 377 (1991),
682 doi:[10.1007/BF00682193](https://doi.org/10.1007/BF00682193).
- 683 [70] P. Bruno, *Absence of spontaneous magnetic order at nonzero temperature in one- and two-*
684 *dimensional heisenberg and xy systems with long-range interactions*, Phys. Rev. Lett. **87**,
685 137203 (2001), doi:[10.1103/PhysRevLett.87.137203](https://doi.org/10.1103/PhysRevLett.87.137203).
- 686 [71] L. Yang, P. Weinberg and A. E. Feiguin, *Topological to magnetically ordered quantum*
687 *phase transition in antiferromagnetic spin ladders with long-range interactions*, SciPost
688 Phys. **13**, 060 (2022), doi:[10.21468/SciPostPhys.13.3.060](https://doi.org/10.21468/SciPostPhys.13.3.060).
- 689 [72] A. Vishwanath, L. Balents and T. Senthil, *Quantum criticality and deconfinement*
690 *in phase transitions between valence bond solids*, Phys. Rev. B **69**, 224416 (2004),
691 doi:[10.1103/PhysRevB.69.224416](https://doi.org/10.1103/PhysRevB.69.224416).
- 692 [73] T. Senthil, A. Vishwanath, L. Balents, S. Sachdev and M. P. A. Fisher, *Deconfined quantum*
693 *critical points*, Science **303**(5663), 1490 (2004), doi:[10.1126/science.1091806](https://doi.org/10.1126/science.1091806).
- 694 [74] T. Senthil, L. Balents, S. Sachdev, A. Vishwanath and M. P. A. Fisher, *Quantum criti-*
695 *cality beyond the landau-ginzburg-wilson paradigm*, Phys. Rev. B **70**, 144407 (2004),
696 doi:[10.1103/PhysRevB.70.144407](https://doi.org/10.1103/PhysRevB.70.144407).
- 697 [75] T. Senthil, L. Balents, S. Sachdev, A. Vishwanath and M. P. A. Fisher, *Deconfined criti-*
698 *cality critically defined*, Journal of the Physical Society of Japan **74**(Suppl), 1 (2005),
699 doi:[10.1143/JPSJS.74S.1](https://doi.org/10.1143/JPSJS.74S.1).
- 700 [76] S. Yang, D.-X. Yao and A. W. Sandvik, *Deconfined quantum criticality in spin-1/2 chains*
701 *with long-range interactions*, doi:[10.48550/ARXIV.2001.02821](https://doi.org/10.48550/ARXIV.2001.02821) (2020).
- 702 [77] K. P. Schmidt and G. S. Uhrig, *Excitations in one-dimensional $s = \frac{1}{2}$ quantum antiferro-*
703 *magnets*, Phys. Rev. Lett. **90**, 227204 (2003), doi:[10.1103/PhysRevLett.90.227204](https://doi.org/10.1103/PhysRevLett.90.227204).
- 704 [78] S. Takada and H. Watanabe, *Nonlocal unitary transformation and haldane state in $s=1/2$*
705 *antiferromagnetic ladder model*, Journal of the Physical Society of Japan **61**(1), 39
706 (1992), doi:[10.1143/JPSJ.61.39](https://doi.org/10.1143/JPSJ.61.39).

- 707 [79] H. Watanabe, *Hidden order and symmetry breaking in the ground state of a*
708 *spin-1/2 antiferromagnetic heisenberg ladder*, Phys. Rev. B **52**, 12508 (1995),
709 doi:[10.1103/PhysRevB.52.12508](https://doi.org/10.1103/PhysRevB.52.12508).
- 710 [80] Y. Nishiyama, N. Hatano and M. Suzuki, *Phase transition and hidden orders of the heisen-*
711 *berg ladder model in the ground state*, Journal of the Physical Society of Japan **64**(6),
712 1967 (1995), doi:[10.1143/JPSJ.64.1967](https://doi.org/10.1143/JPSJ.64.1967).
- 713 [81] S. R. White, *Equivalence of the antiferromagnetic heisenberg ladder to a single $s=1$ chain*,
714 Phys. Rev. B **53**, 52 (1996), doi:[10.1103/PhysRevB.53.52](https://doi.org/10.1103/PhysRevB.53.52).
- 715 [82] E. H. Kim, G. Fáth, J. Sólyom and D. J. Scalapino, *Phase transitions between topologi-*
716 *cally distinct gapped phases in isotropic spin ladders*, Phys. Rev. B **62**, 14965 (2000),
717 doi:[10.1103/PhysRevB.62.14965](https://doi.org/10.1103/PhysRevB.62.14965).
- 718 [83] Y. Nambu, *Quasi-particles and gauge invariance in the theory of superconductivity*, Phys.
719 Rev. **117**, 648 (1960), doi:[10.1103/PhysRev.117.648](https://doi.org/10.1103/PhysRev.117.648).
- 720 [84] J. Goldstone, *Field theories with « superconductor » solutions*, Il Nuovo Cimento (1955-
721 1965) **19**(1), 154 (1961), doi:[10.1007/BF02812722](https://doi.org/10.1007/BF02812722).
- 722 [85] J. Goldstone, A. Salam and S. Weinberg, *Broken symmetries*, Phys. Rev. **127**, 965 (1962),
723 doi:[10.1103/PhysRev.127.965](https://doi.org/10.1103/PhysRev.127.965).
- 724 [86] O. K. Diessel, S. Diehl, N. Defenu, A. Rosch and A. Chiocchetta, *Generalized higgs mech-*
725 *anism in long-range interacting quantum systems*, doi:[10.48550/ARXIV.2208.10487](https://doi.org/10.48550/ARXIV.2208.10487)
726 (2022).
- 727 [87] C. Knetter and G. S. Uhrig, *Perturbation theory by flow equations: dimerized and frus-*
728 *trated $S=1/2$ chain*, Eur. Phys. J. B **13**(2), 209 (2000), doi:[10.1007/s100510050026](https://doi.org/10.1007/s100510050026).
- 729 [88] C. Knetter, K. P. Schmidt and G. S. Uhrig, *The structure of operators in effective*
730 *particle-conserving models*, J. Phys. A **36**(29), 7889 (2003), doi:[10.1088/0305-](https://doi.org/10.1088/0305-4470/36/29/302)
731 [4470/36/29/302](https://doi.org/10.1088/0305-4470/36/29/302).
- 732 [89] K. Coester and K. P. Schmidt, *Optimizing linked-cluster expansions by white graphs*, Phys.
733 Rev. E **92**, 022118 (2015), doi:[10.1103/PhysRevE.92.022118](https://doi.org/10.1103/PhysRevE.92.022118).
- 734 [90] S. Sachdev, *Quantum Phase Transitions*, Cambridge University Press, ISBN
735 9781139500210 (2011).
- 736 [91] M. E. Fisher, S.-k. Ma and B. G. Nickel, *Critical exponents for long-range interactions*,
737 Phys. Rev. Lett. **29**, 917 (1972), doi:[10.1103/PhysRevLett.29.917](https://doi.org/10.1103/PhysRevLett.29.917).
- 738 [92] J. Sak, *Low-temperature renormalization group for ferromagnets with long-range inter-*
739 *actions*, Phys. Rev. B **15**, 4344 (1977), doi:[10.1103/PhysRevB.15.4344](https://doi.org/10.1103/PhysRevB.15.4344).
- 740 [93] F. Pollmann, E. Berg, A. M. Turner and M. Oshikawa, *Symmetry protection of topologi-*
741 *cal phases in one-dimensional quantum spin systems*, Phys. Rev. B **85**, 075125 (2012),
742 doi:[10.1103/PhysRevB.85.075125](https://doi.org/10.1103/PhysRevB.85.075125).
- 743 [94] J. Koziol, S. Fey, S. C. Kapfer and K. P. Schmidt, *Quantum criticality of the transverse-field*
744 *Ising model with long-range interactions on triangular-lattice cylinders*, Phys. Rev. B **100**,
745 144411 (2019), doi:[10.1103/PhysRevB.100.144411](https://doi.org/10.1103/PhysRevB.100.144411).

- 746 [95] S. Sachdev and R. N. Bhatt, *Bond-operator representation of quantum spins: Mean-field*
747 *theory of frustrated quantum heisenberg antiferromagnets*, Phys. Rev. B **41**, 9323 (1990),
748 doi:[10.1103/PhysRevB.41.9323](https://doi.org/10.1103/PhysRevB.41.9323).
- 749 [96] M. Hörmann, P. Wunderlich and K. P. Schmidt, *Dynamic structure factor*
750 *of disordered quantum spin ladders*, Phys. Rev. Lett. **121**, 167201 (2018),
751 doi:[10.1103/PhysRevLett.121.167201](https://doi.org/10.1103/PhysRevLett.121.167201).
- 752 [97] C. J. Hamer, W. Zheng and R. R. P. Singh, *Dynamical structure factor for the alternat-*
753 *ing heisenberg chain: A linked cluster calculation*, Phys. Rev. B **68**, 214408 (2003),
754 doi:[10.1103/PhysRevB.68.214408](https://doi.org/10.1103/PhysRevB.68.214408).
- 755 [98] G. Baker, *Essentials of Padé Approximants*, Elsevier Science, ISBN 9780323156158
756 (1975).
- 757 [99] A. J. Guttmann, *Asymptotic Analysis of Power-Series Expansions*, In C. Domb, M. S. Green
758 and J. L. Lebowitz, eds., *Phase Transitions and Critical Phenomena*, vol. 13. Academic
759 Press (1989).
- 760 [100] F. J. Wegner and E. K. Riedel, *Logarithmic corrections to the molecular-field behavior of*
761 *critical and tricritical systems*, Phys. Rev. B **7**, 248 (1973), doi:[10.1103/PhysRevB.7.248](https://doi.org/10.1103/PhysRevB.7.248).
- 762 [101] R. Bauerschmidt, D. C. Brydges and G. Slade, *Scaling limits and critical behaviour of the*
763 *4-dimensional n -component $|\varphi|^4$ spin model*, Journal of Statistical Physics **157**(4),
764 692 (2014), doi:[10.1007/s10955-014-1060-5](https://doi.org/10.1007/s10955-014-1060-5).
- 765 [102] M.-w. Xiao, *Theory of transformation for the diagonalization of quadratic hamiltonians*,
766 doi:[10.48550/ARXIV.0908.0787](https://doi.org/10.48550/ARXIV.0908.0787) (2009).
- 767 [103] M. E. Fisher, *The renormalization group in the theory of critical behavior*, Rev. Mod. Phys.
768 **46**, 597 (1974), doi:[10.1103/RevModPhys.46.597](https://doi.org/10.1103/RevModPhys.46.597).
- 769 [104] M. E. Fisher, *Scaling, universality and renormalization group theory*, In F. J. W. Hahne,
770 ed., *Critical Phenomena*, pp. 1–139. Springer Berlin Heidelberg, Berlin, Heidelberg,
771 ISBN 978-3-540-38667-4 (1983).
- 772 [105] K. Binder, *Finite size effects on phase transitions*, Ferroelectrics **73**(1), 43 (1987),
773 doi:[10.1080/00150198708227908](https://doi.org/10.1080/00150198708227908).
- 774 [106] B. Berche, R. Kenna and J.-C. Walter, *Hyperscaling above the up-*
775 *per critical dimension*, Nuclear Physics B **865**(1), 115 (2012),
776 doi:<https://doi.org/10.1016/j.nuclphysb.2012.07.021>.
- 777 [107] Kenna and Berche, *A new critical exponent ν and its logarithmic counterpart ν_{log}*
778 *hat*, Condensed Matter Physics **16**(2), 23601 (2013), doi:[10.5488/cmp.16.23601](https://doi.org/10.5488/cmp.16.23601).